Hindawi
International Journal of Intelligent Systems
Volume 2024, Article ID 6678384, 29 pages
https://doi.org/10.1155/2024/6678384

Research Article

Comparison of Bioinspired Techniques for Tracking Maximum Power under Variable Environmental Conditions

Dilip Yadav,[1] **Nidhi Singh**,[1] **Nimay Chandra Giri**,[2] **Vikas Singh Bhadoria**,[3] **and Subrata Kumar Sarker**[4]

[1]*Electrical Engineering Department, Gautam Buddha University, Greater Noida, Uttar Pradesh 201312, India*
[2]*Department of Electronics and Communication Engineering, Centurion University of Technology and Management, Jatni 752050, Odisha, India*
[3]*IIC, Shri Vishwakarma Skill University, Palwal, Haryana 121102, India*
[4]*Department of Mechatronics Engineering, Rajshahi University of Engineering and Technology, Rajshahi, Bangladesh*

Correspondence should be addressed to Subrata Kumar Sarker; subrata@mte.ruet.ac.bd

Received 17 June 2023; Revised 25 January 2024; Accepted 22 March 2024; Published 12 April 2024

Academic Editor: Alexander Hošovský

This paper presents a comparative analysis of bioinspired algorithms employed on a PV system subject to standard conditions, under step-change of irradiance conditions, and a partial shading condition for tracking the global maximum power point (GMPP). Four performance analysis and comparison techniques are artificial bee colony, particle swarm optimization, genetic algorithm, and a new metaheuristic technique called jellyfish optimization, respectively. These existing algorithms are well-known for tracking the GMPP with high efficiency. This paper compares these algorithms based on extracting GMPP in terms of maximum power from a PV module running at a uniform (STC), nonuniform solar irradiation (under step-change of irradiance), and partial shading conditions (PSCs). For analysis and comparison, two modules are taken: 1Soltech-1STH-215P and SolarWorld Industries GmbH Sunmodule plus SW 245 poly module, which are considered to form a panel by connecting four series modules. Comparison is based on maximum power tracking, total execution time, and minimum number of iterations to achieve the GMPP with high tracking efficiency and minimum error. Minitab software finds the regression equation (objective function) for STC, step-changing irradiation, and PSC. The reliability of the data (P-V curves) was measured in terms of p value, R, R^2, and VIF. The R^2 value comes out to be near 1, which shows the accuracy of the data. The simulation results prove that the new evolutionary jellyfish optimization technique gives better results in terms of higher tracking efficiency with very less time to obtain GMPP in all environmental conditions, with a higher efficiency of 98 to 99.9% with less time of 0.0386 to 0.1219 sec in comparison to ABC, GA, and PSO. The RMSE value for the proposed method JFO (0.59) is much lower than that of ABC, GA, and PSO.

1. Introduction

Photovoltaic (PV) technology is a promising one that sees annual capacity growth around the globe as it is a clean and convenient energy source. In recent years, renewable energy sources, such as solar, tidal, biogas, wind, and solar power, have become essential for power generation [1, 2]. One such potential innovation is the solar cell, which transforms solar energy into electrical energy that can be used directly in various ways. Although solar or PV cells are beneficial, they cannot convert all sun energy into electricity. Conversion efficiency refers to the proportion of solar energy a PV device turns into useable power [3]. The MPP is often reached by modifying the PV panel power, which is a function of voltage and current. Power electronic converters (DC-DC converters) [4] are vital in stabilizing the voltage in all conditions. According to the authors in [5], there are two types of MPPT control methods for PV systems: traditional methods and soft-computing approaches, which are further subdivided into artificial intelligence, bionature-inspired, and

swarm-based MPPT techniques. Soft-computing, artificial intelligence (AI), and bioinspired (BI) techniques are the most powerful methods of tracking MPP, and they are highly effective and highly efficient when it comes to multi-constraint issues in solar PV optimization [3, 6]. Conventional MPPT algorithms fail to find the maximum point when environmental factors repeatedly vary; therefore, they are suitable for low-power and high-power applications [7]. The P-V characteristic curve exhibits a nonlinear, time-varying MPP problem due to the sudden changes in environmental variables, namely, sun irradiance and temperature. To overcome the problem of the conventional method, artificial intelligence was introduced, which could deal with the nonlinear behavior occurring in the PV system; moreover, they did not rely on the model or PV features. They could even use online follow-ups and self-learning to improve the algorithm [6, 7]. However, they are complex, costly, and take longer to determine the MPP. These MPPT algorithms are, unfortunately, more expensive to implement than traditional ones and need a specific training dataset.

Heuristic optimization methodologies are becoming more common as they can handle the challenges of traditional and AI-based. Moreover, bioinspired algorithms [8] involve fewer computations than AI algorithms. These heuristic approaches are beneficial and effective in finding the optimal solution for complicated problems in science and engineering, and they often do not need extensive mathematical expertise. Different applications of optimization techniques in variousfields of engineering are discussed in [8]. A few MPPT approaches have been suggested [6–8] and used recently to improve the PV yield under various atmospheric conditions. According to the authors in [9], MPPT problems are typically solved by considering five different techniques: the first approach employs techniques that consider constant variables, such as the PV current linear relationship with the short-circuit current; the traditional perturb and observe (P and O) strategy and its modified tactics are used in the second method, which involves the trial-and-error process; the third utilises comparison and measurement techniques, particularly the look-up table method; and the fourth employs mathematically based computation techniques such as incremental conductance (INC), while the last approach makes use of soft-computing techniques such as particle swarm optimization (PSO) or fuzzy logic controller (FLC) [6]. Bioinspired algorithms, such as swarm insight (SI) methodologies [6–9], have gained increased recognition as excellent optimization strategies for delivering the best responses and solving challenging issues during the PSC. The authors in [10] have given the classification of a few well-known MPP controllers with the advantages and disadvantages of conventional and optimization algorithms.

The classification of different algorithms is illustrated in Figure 1. A few of the well-known optimization techniques are artificial immune system (AIS) [8], ant colony optimization (ACO) [5, 8, 12–14], moth-flame optimization (MFO) [12, 15], whale optimization algorithm (WOA) [12], butterfly optimization (BFO) algorithm [12], shuffled frog leaping algorithms (SFLA) [12], slap swarm algorithm [12], firefly algorithm (FA) [12, 16, 17], artificial bee colony (ABC) [5, 8, 9, 12, 13, 16–20], bat-search algorithm (BA) [12, 17], grey wolf optimization (GWO) [5, 12, 13, 15, 17, 21, 22], genetic algorithm (GA) [8, 12–14, 21, 23], flower pollination optimization (FPO) [12, 16, 24], JAYA [16], DE [8, 16], cuckoo search (CS) [5, 6, 12, 13, 15, 16, 24], particle swarm optimization (PSO) [5, 6, 8, 13–17, 19–29], seagull optimization algorithm (SOA) [27], Harris hawk optimization (HHO) [16, 20], African vultures optimization algorithm (AVOA) [30], AOA-based PI-IC-MPPT [21], grasshopper optimization algorithm (GOA) [15], Aquila optimizer (AO) [21], antlion optimizer (ALO) [21], tuna swarm optimization (TSO) [21], black widow spider (BWS), squirrel search algorithm (SSA) [15], yellow saddle goatfish algorithm (YSGA), and butterfly optimization algorithm (BOA) [29]. These are optimization techniques that have been utilized for comparing different factors in terms of tracking time [16, 21, 24, 29], tracking efficiency [13, 14, 16, 20, 22, 24, 29, 31], root mean square error [12, 14, 15, 18, 20], and mean absolute error [20]. Some of the new optimization techniques that have been recently introduced in the PV system analysis in 2022 and 2023 are specified as seagull optimization algorithm [27], African vulture optimization [30], jellyfish optimization algorithm [32], arithmetic optimization algorithm [21], reptile search algorithm [22], particle swarm optimization with butterfly optimization algorithm [29], DGBCO [33], EVO [34], GRNN-OPA [35], MRO [36], and many others that are utilized in different fields of engineering.

A Google Scholar study was conducted during the past five years, 2015–2020, on nonuniform solar irradiance and shading conditions [23]. Evolutionary algorithms (EAs) have emerged as the frontrunner for MPP tracking problems under shading circumstances [25]. These algorithms confirm that the PV system always runs at its GMPP, regardless of the change in the atmospheric condition (irradiation and temperature). Several approaches fail to determine the global point because they get trapped in local points or local maxima and minima. The paper [23, 24] focuses on classifications of optimization techniques, mathematical expressions, operational principles, and flowcharts [26]. This paper presents an attempt to highlight the present and future problems associated with developing high-performance PV systems. The determination of numerous parameters might cause the optimization approach to become challenging or complicated [27]. The literature research on finding popular optimization approaches is shown in Table 1. According to the authors in [20], the PSO gives optimum efficiency even under PSC, but it quickly falls into local optima, and as a result, determining MPP takes a long time. ABC has a strong exploration ability to follow MPP, though these approaches are highly prone to exploitation. [37] gives the modeling [38], electrical characteristics, and [39] parameter estimation of photovoltaic strings under PSC and explains the importance of bypass diodes The authors in [15, 19, 40–42] has reviewed and compared the performance of some well-known optimization algorithms under partially shaded conditions. The authors in [13] have reviewed and given the performance comparisons of conventional,

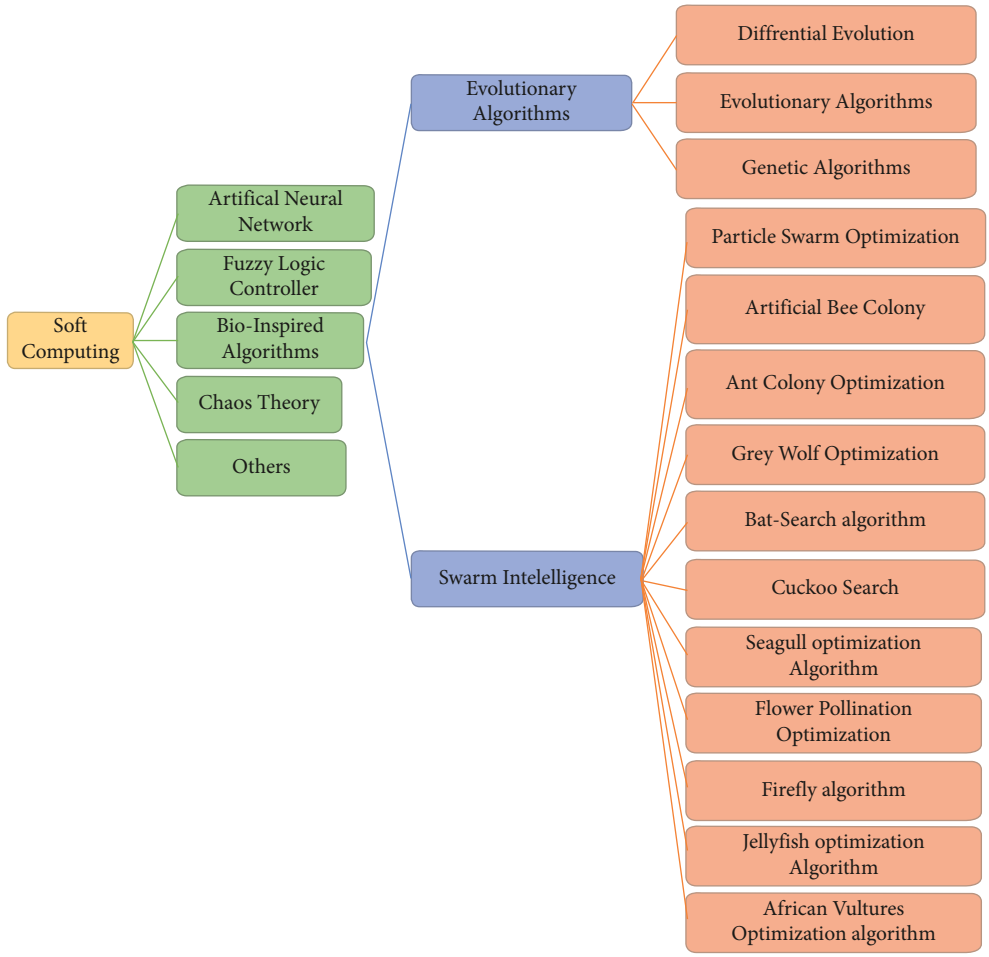

Figure 1: Classification of different algorithms [11].

artificial intelligence, and optimization-based MPPT in terms of tracking capability, convergence, implementation, tracking accuracy, tracking speed, efficiency, economy, and application and have given advantages and disadvantages of different optimization techniques used to track the GMPP. In [43], a comprehensive comparative analysis of the twenty-eight adaptive MPPT algorithms is performed based on the tracking time, steady-state oscillations, conversion efficiency, algorithm complexity, implementation cost, and the capability to perform on the partial shading conditions. This will help the readers to select the suitable MPPT methods. The authors in [44] focused on the use of jellyfish search optimizer in solving optimization problems. The authors in [32] have given a detailed explanation of the jellyfish optimization algorithm with its application in engineering. The authors in [11, 14] have shown a comparison of the different optimization techniques [28]. PSO and FPA are compared with ten (10) samples for PSC and it is concluded that the FPA produces 86.03 W power output compared to the power output in PSO of 85.5 W under PSC in the PV panel. The authors in [21] introduced AOA-based PI-IC-MPPT, which gives better results than MIC, GWO, GA, and PSO in terms of reducing rise time and settling time. The authors in [22] used the RAS optimization technique and proved that RSA gives better efficiency than DOA, GWO, WOA, and PSO. The authors in [29] used hybrid methods such as BOA-PSO-based algorithm and found that the PSO-BOA algorithm outperforms the PSO and BOA in terms of convergence accuracy, with a tracking accuracy of not less than 99.94%. The authors in [33] concluded that DGBCO has significantly less RMSE value than other algorithms. The authors in [45] reviewed some algorithms and proposed a SHTS algorithm that was compared with hybrid algorithms in terms of tracking speed and accuracy under partial shading conditions. Hybrid IABC + SHTS performs excellently in precisely identifying the GMPP of PV systems with phenomenal rapidity among multiple peaks. The authors in [34] introduced the energy valley optimizer (EVO) MPPT algorithm, showcasing 30% quicker tracking and 80% faster settling time. Research [35] also highlights the GRNN-OPA-based MPPT's superior performance with 35% faster tracking, 90–110% quicker settling time, and 4–8% higher energy accumulation. In [36], the proposed controller achieves an average of 99.95% power output and 220 ms response time under dynamic thermal conditions, demonstrating 38–70% faster tracking of the maximum power point in dynamic operating conditions.

Table 1: Literature review based on RMSE.

Reference	Year	Method	Finding	RMSE
[18]	2021	ABC and P and O	ABC archives a much superior performance than P and O	*RMSE* ABC = 0.72, P and O = 0.919
[20]	2023	TLABC, PSO, and ABC	TLABC < PSO < ABC	*MAE* = 0.13 Efficiency = 99.89%
[15]	2022	PSO, CSA, GWO, MFO, WOA, SSA, and GOA	RMSE of GOA and WOA is less than the rest of the algorithms, which means that the power tracked by these algorithms is dense around the GMPP	*RMSE* GOA = 3.9 SSA = 8.8 WOA = 3.9 MFO = 8.5 GWO = 6.8 CSA = 11 PSO = 11.6
[14]	2020	ACO, GA, and PSO	PSO-based optimization attains higher tracking efficiency than GA	*RMSE* ACO = 0.0021 GA = 0.0010 PSO = 0.0012
[33]	2022	DGBCO, DFO, ABC, CS, and PSO	DGBCO < DFO < ABC < CS < PSO	*RMSE* DGBCO = 0.55 DFO = 0.588 ABC = 0.771 CS = 0.877 PSO = 0.947

Many researchers [31, 46] have used regression analysis for forecasting PV power and concluded that one of the convenient ways to model PV performance is linear regression models. A multiple linear regression model was implemented for PV systems for MPPT, and regression analysis of a photovoltaic system in terms of RMSE was considered to generate the regression coefficient. The authors in [46] have given the application of regression analysis and machine learning for tracking the maximum power and the performance analysis of PV modules using regression analysis. According to the authors in [31], the accuracy obtainable for the prediction will depend on the value of the parameter R^2, which lies between 0 and 1. The closer the value of R^2 to 1, the more accurately the PV module regression model is predicted to function [31, 46].

This paper uses a new metaheuristic JFO algorithm to track the PV panel's GMPP with the help of regression analysis of the PV curve obtained by P-V curves. The objective function equation is formulated by using the regression analysis with the help of the Minitab software. The equation comprises of correlation factors that determine the power voltage and current relationship. This equation is optimized by using the JFO to find the voltage and current's value corresponding to GMPP. Many authors [6, 10, 12, 16–19, 22, 23, 27, 29, 31, 43] have compared algorithms based on tracking capability, total execution time, tracking efficiency [16, 29], and accuracy. The authors in [25] compared in terms of population size, [14, 24] compared in terms of Iteration. The authors in [7] analysed the performance at different irradiation and PSC. Refrences [12, 14, 15, 18, 20, 33] compared RMSE and, the authors in [20] in terms of MAE. In this paper, three cases, STC, step-changing irradiation, and PSC, are taken to validate the performance of JFO in terms of maximum power tracking, total execution time, the minimum number of iterations to achieve the GMPP with high tracking efficiency, and RMSE for the same set of population and number of iterations. The analysis and comparison between the existing techniques (GA, ABC, and PSO) and the proposed technique (JFO) is carried out with a smaller population size ($N_{pop} = 8$) and maximum iterations ($Ite_{Max} = 100$). The module parameters, specification, irradiation, and temperature are kept the same for all cases. Also, the effect of air mass, wind, module heating, soiling, panel orientation, and humidity has not been considered in this research.

Section 2 briefly introduces the PV system description with the PV panel's main equations, explains different optimization techniques with the flowchart, thoroughly explains how the JFO method works, and illustrates the critical phases in its execution. Finally, Section 3 gives the process of objective function formation with the help of Minitab software (regression model) in which power was made a function of voltage and current with coefficients that describe the P-V curve of the PV system for different environmental conditions, i.e., at STC, step-changing irradiations, and PSC. The MATLAB/simulation software was used to find the response of other optimization techniques. The results obtained in both case studies (1Soltech-1STH-215P and SolarWorld Industries GmbH Sunmodule plus SW 245 poly module) are compared with other optimization algorithms, i.e., PSO, GA, ABC, and JFO-based optimization at STC, step-changing irradiation, and PSC conditions for the same set of iterations and population size. Lastly, a comparison between the proposed technique and other optimization techniques is made. The results prove that the JFO-based optimization technique gives the desired output with less population and in less time with higher efficiency and lowest RMSE value. These findings and problem-solving techniques prove the novelty of the paper and JFO algorithm. Finally, conclusions are drawn in Section 4.

2. Materials and Methods

A photovoltaic cell is an energy-harvesting technology that converts solar energy into practical electricity through a photovoltaic effect [37]. The smallest unit is called a solar cell, the arrangement of cells in series and parallel combination forms module, arrangement of modules into series or parallel combination form panel, and a combination of modules form array. Irradiation and temperature significantly impact the performance of PV power generation, as solar irradiation is nonuniform in real life [38]. Tracking the real MPP is thus a crucial factor to consider while choosing the technique. The complexity of an algorithm's design and efficiency significantly impacts how accurate and efficient the optimization techniques used for tracking GMPP are. The PV system's constant steady-state response, tracking time, and efficiency were the primary deciding factors while evaluating the different optimization techniques. Considering all these factors, the design parameters of the PV module and other optimizations are illustrated in the subsections given as follows.

2.1. PV System Description. An antiparallel diode coupled to series resistance (R_s) and parallel resistance (R_{sh}) is used to represent the equivalent circuit of a single-diode PV cell (see Figure 2). The photovoltaic current generated (I_{pv}) is expressed as [27, 37] follows:

$$I_{pv} = I_{Ph} - I_0 * \left[\exp\left(\frac{V_{pv} + I_{pv} R_s}{N_s * (\mathbf{k} * \alpha * \mathbf{T}/\mathbf{q})} \right) - 1 \right] - \frac{V_{pv} + I_{pv} R_s}{R_{sh}}. \quad (1)$$

The total module current is calculated by using equation (1), where I_{pv} is the module current, V_{pv} is the module voltage, I_{ph} is the photogenerated current, I_0 is the diode reverse saturation current, I_{sh} is the current through shunt resistance, R_s is the series resistance, R_{sh} is the shunt resistance, N_s is the number of cells, V_t is the junction's

thermal voltage and can be expressed as $V_T = (k * \alpha * T)/q$, where k is the Boltzmann's constant 1.38×10^{-2} J/K, q is the electron charge equal to 1.602×10^{-19} C, T is the temperature in kelvin, and α is the ideality factor constant [44], and $I_{\text{Ph}} = (G/G_{\text{ref}})\ [I_{\text{SC,Ref}} + \mu_{\text{SC}}\ (T - T_{\text{Ref}})]$, where $I_{\text{sc,ref}}$ is the solar cell short-circuit current, $G_{\text{ref}} = 1000\ \text{W/m}^2$, $T_{\text{ref}} = 25^{\circ}\text{C}$, μ_{SC} is the solar cell short-circuit temperature coefficient, usually provided by the manufacturer (A/K), and G is the actual irradiance intensity (W/m^2) [27].

When PV modules are exposed to high solar irradiation and low solar irradiation, they produce less current than unshaded modules, resulting in a phenomenon known as mismatch loss, which is also known as the partial shading condition (PSC). PSC affects the electrical characteristics of PV strings, so bypass diodes are coupled in parallel to every module to prevent this mismatch loss. The following equation [16] represents the bypass diode's reverse bias saturation current ($I_{\text{sat,bp}}$) computed:

$$I_{\text{bp}} = I_{\text{sat,bp}} * \left[\exp\left(\frac{V_s}{N_s * (k * \alpha * T/q)} \right) - 1 \right]. \tag{2}$$

The simulation model is designed in MATLAB software to form a panel by combining four series modules (Figure 3(a)) that are connected by a bypass diode [38]. In PV modules, bypass diodes are utilized to avoid generating an excessive reverse voltage across the cells in the presence of shading. When one or more PV system cells are shaded and receive different solar radiation, it results in a partial shading condition [38]. The shadows projected by nearby trees, clouds, buildings, dust, and bird droppings are some causes of shading conditions. A frequent change in the irradiation level can permanently harm PV modules by generating cell mismatches, hotspots, and unexpected system losses in the PV system. Such a problem in the PV system can be avoided by connecting it to the PV module with a bypass diode. The P-V curve produced by these diodes exhibits various power peaks (Figure 3(b)), known as LMPP and GMPP.

2.2. Different Algorithms for Tracking GMPP. Solving challenging mathematical puzzles in various domains is one of the most difficult tasks for a human being. Nature is one of the excellent and extensive sources of inspiration that help lead the way in solving these complex problems efficiently. Optimization problems should keep the balance between the dependent variables while defining the objective functions. Many optimization methods have proved their importance in solving nondifferentiable and discontinuous problems in solar power generation to track the GMPP during the PSC and under step-change of irradiance conditions [6–10, 12, 16–20, 23–27, 30]. Due to some advantages [37] over conventional methods and intelligent techniques, heuristic approaches are usually used in the paper as they can quickly adapt to algorithm changes, and ample space for possible optimal solutions is available for different problems.

PSO [5, 6, 8, 11, 13, 14, 16, 17, 19, 23–26], GA [8, 11–14, 23], and ABC [5, 8, 11–13, 16–19] are the most widely used optimization algorithms because of some

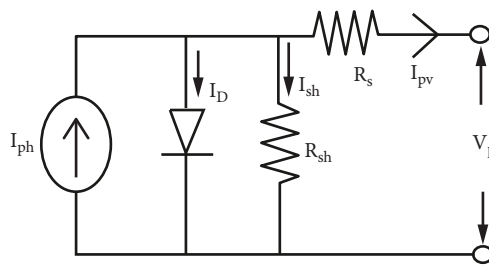

Figure 2: Single-diode PV cell equivalent circuit diagram [2].

advantages [5, 16, 17] such as their simple structure, independence of a mathematical model, capability to solve nonlinear and challenging mathematical problems, easy understanding, and high reliability. Each optimization technique considers a few deciding factors such as the number of populations and a few particles/food sources/chromosomes/jellyfish. The stopping criteria of each optimization technique are based on the previous best optimal solution compared with the current optimal solution such that the current solution should be greater than the last optimal solution value. The optimal solution can be in terms of $P_{\max}$ or less error or any parameter (cost function) that can be maximized or minimized. Each algorithm has some stopping criterion that helps determine the problem's optimal solution. Root mean square error (RMSE) is an essential metric for assessing the effectiveness of MPPT methodologies. The following equation is used for this statistical analysis [33, 34].

$$\text{Error}_{\text{RMSE}} = \sqrt{\frac{\sum_{i=1}^{n} \left(P_{\text{pvi}} - P_{\text{pvi}} \right)^2}{n}}, \tag{3}$$

where P_{pvi} represents the power at STC, P_{pv} is the power tracked, and n represents the number of samples.

Regression analysis is a statistical approach that obtains the best coefficients to model the system with a minimum cumulative least square error. The accuracy obtainable for the prediction will depend on the value of the parameter R^2, which lies between 0 and 1, and the nearer this value is to 1, the better the predicted accuracy of the regression model designed for the PV module [31, 46]. P value is a statistical test that determines the probability of extreme results of the statistical data where its coefficient turns out to be zero, i.e., for a lower value of <0.05 [31]. In the literature, some researchers have tried to apply linear regression to model PV systems. The goodness R^2 of fit is defined as [46] follows:

$$R^2 = 1 - \frac{\sum_{k=1}^{ns} \left(Y_i - Yo \right)^2}{\sum_{k=1}^{ns} \left(Y_i - Y_a \right)^2}, \tag{4}$$

where Y_a is the mean value of Y_i and ns is the sample count. The value of R^2 and RMSE closer to zero represents the model with greater prediction strength [46].

A multiple linear regression model for PV can be denoted as follows [31]:

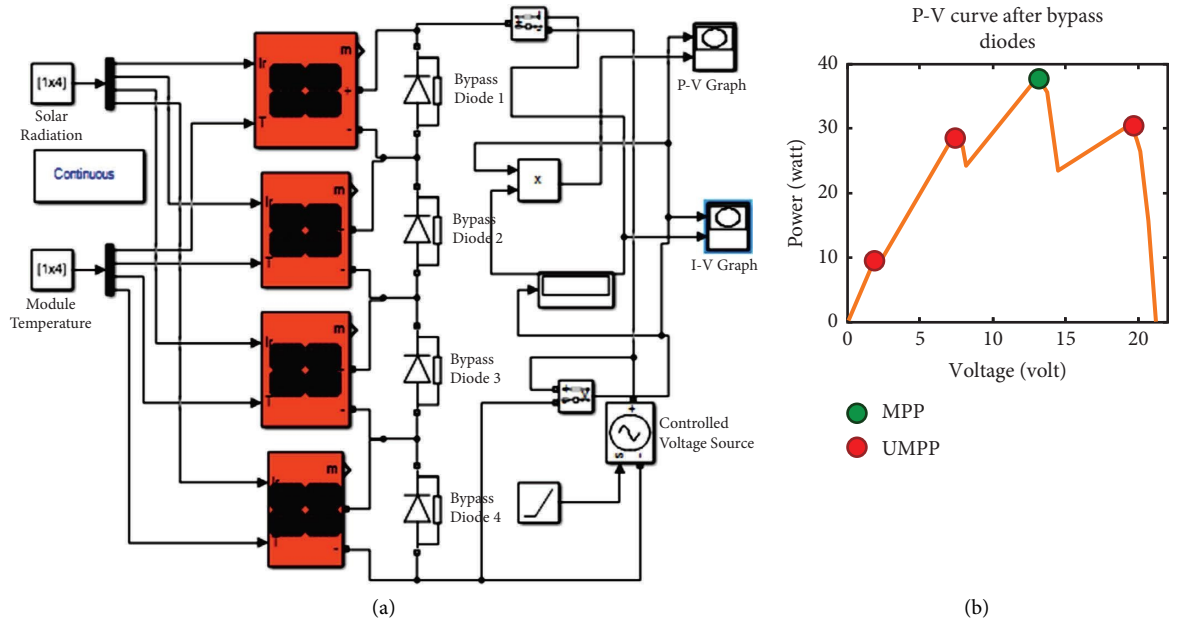

Figure 3: (a) Panel (four series module) and (b) P-V curve at PSC.

$$y = \beta_0 + \beta_1 v_1 + \beta_2 v_2 + \beta_3 v_3 + \cdots\cdots + \beta_n v_n + e, \quad (5)$$

where v_1 and v_2, ..., are the input variables (1 to n). The coefficient is the intercept, while values of β_n, ..., denote the slope coefficient of each input (explanatory) variable and the error e (the amount by which the predicted value is different from the actual value). The regression model estimates the best values, leading to the least error "R." R is known as the correlation coefficient, and its value determines the strength and direction of linear association between the two variables under examination. Building a model with a small dataset and a high number of predictors leads to a model with low performance, and the correlation between predictors could increase, leading to high values of VIF (variance inflation factor) for predictors [31]. A VIF of <5 for their predictors makes them the potential models for independent variables. The collinearity of variables is checked through the VIF. The VIF of a predictor is low when it is <5, and the VIF of a predictor is moderate when it is <10 [31]. The values of the correlation coefficient R near 1 or 1 indicate a strong correlation between the two variables. In this paper, the value of R is 0.95, which shows the excellent correlation between the variables V and I with P_{max}. After using the regression analysis of the PV curve, an objective function is formed that is tested by calculating its RMSE value.

Different algorithms can find the GMPP at STC, under step-changing irradiation, and PSC [8–20, 23–27, 30, 37–43]. Artificial jellyfish optimization (JFO) [44] is a new novel swarm-based optimization algorithm with some advantages over other algorithms. JFO can balance exploration and exploitation strategies well and reach optimal solutions in less time [32, 44]. A comparative analysis is performed for the two panels for STC, step-change of irradiances, and PSC conditions. JFO is compared among the PSO, ABC, and GA. A brief introduction of these algorithms is as follows.

2.2.1. Genetic Algorithm (GA). It is one of the most influential evolutionary algorithms based on the theory that living things have evolved biologically and Darwin's principle of "survival of the fittest" [8]. A function optimizer is another name for it [12, 23]. GA commonly uses a fixed population size. Three genetic processes are employed: mutation, crossover, and selection. The process begins with developing a random population of solutions, after which it uses the fitness function or objective function to assess the fitness of each *chromosome*. Then, the best chromosome is picked for the mating pool, and a new set of solutions known as offspring are produced when these chromosomes encounter cross-over and mutation (switches from 1 to 0). To improve the solution selected from the present generation, we choose the most suitable offspring to transmit to future generations. The method is repeated until the requirements are met (P_{max}). Finally, the overview of the genetic algorithm's [8, 12, 13, 23] working principle is displayed in Figure 4(a) [13].

2.2.2. Artificial Bee Colony (ABC). Karaboga proposed the artificial bee colony (ABC) method to optimize numerical challenges in 2005 [17, 44]. The ABC algorithm is a swarm-based metaheuristic algorithm. It was influenced by how honeybees used intelligence in their foraging. The algorithm is based explicitly on the model used for honeybee colony foraging behavior [5, 8, 12, 16–19]. Its operation is based on three phases [17]: the employed bee's phase, the onlooker bee's phase, and the scouting phase. The ABC working method is shown in Figure 4(b).

In ABC, the artificial bees update each position over time using equation (6). The bee's primary goal is finding the best food source to produce the most nectar [8]. Then, the scout bees randomly pick the food sources and fly around the searched area. Finally, the observing bees choose the food source based on the expected amount of nectar [16].

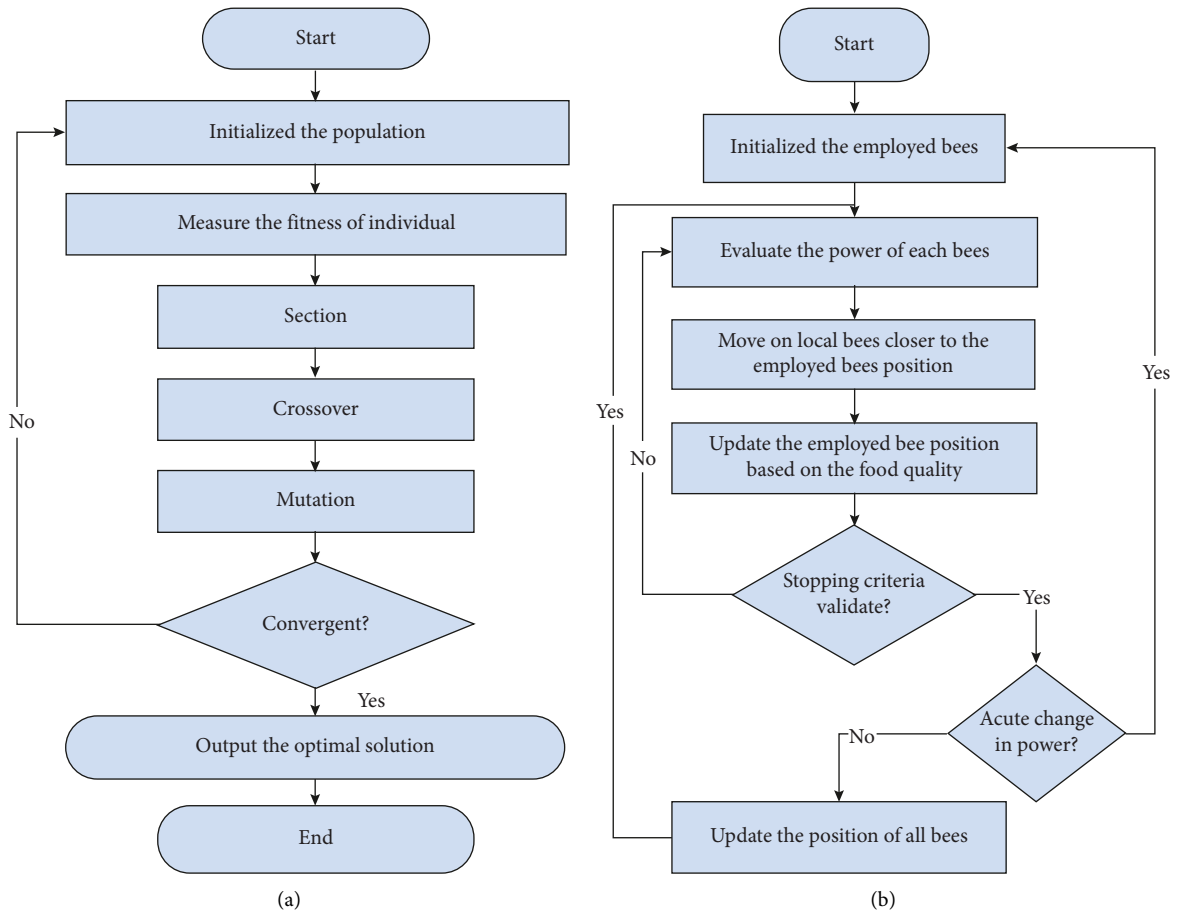

Figure 4: The block diagram of (a) GA [13] and (b) ABC-based optimization technique [13].

They only consider the location of the leading food source during the greedy search process. Whenever a food source is fully utilized, an employed bee transforms into a scout bee and investigates a new area. While creating a new position, the position that best matches the previously created one is chosen. In equation (6) [16], i^{th} is the food source in the swarm (x_i), where $x_{\max j}$ and $x_{\min j}$ are the bounds in the j^{th} dimension and a random number (rand) range from 0 to 1.

$$x_{ij} = x_{\min j} + \text{rand}[0,1]. * \left(x_{\max j} - x_{\min j}\right). \tag{6}$$

The dependency of random food source (r_m) is on selection probability (P_m) that is represented in terms of food source (x_m) with the food source number (F_n) given in the following equation [16]:

$$P_m = \frac{\text{Fitness}\,(x_m)}{\sum_i^{Fn} \text{fitness}\,(x_i)}. \tag{7}$$

By comparing a probability factor associated with several food areas, the location of the food source is determined [5]. The primary objective of the algorithm is to substitute a source of nectar with a higher level of food source. The main advantages are simplicity, high flexibility, strong robustness, few control parameters, ease, and combination with other methods.

2.2.3. Particle Swarm Optimization (PSO). V. Kennedy and Eberhart gave this algorithm structure in 1995 [16]. Like many optimization algorithms, PSO draws inspiration from the natural life cycle and the behaviors during this period. Fish, insect, and bird herd behavior were studied during the development of the PSO and incorporated into the algorithm. Every *particle* has a velocity updating equation (8) and location updating equation (9), resulting in a change in variable according to the local best solution $P_{\text{best},i}$ and the globally best solution G_{best}, which are modified after each iteration by learning from the local best point [12, 16, 17, 23–26]. The PSO working flowchart is given in Figure 5(a). Each particle's position refers to a set point for a variable. The best position is identified by using the following equation [23]:

$$x_i^{t+1} = V_i^{t+1} + x_i^t, \tag{8}$$

where v_i is the velocity component used to represent the MPPT step size. The value of V_i^{t+1} is calculated by using the following equation [23]:

$$V_i^{t+1} = wv_i^t + c_1 r_1\left(P_{\text{best},i} - x_i^t\right) + c_2 r_2\left(G_{\text{best}} - x_i^t\right), \tag{9}$$

where V_i^{t+1} is the velocity of the i^{th} swarm, w is the learning factor, and c_1, c_2, r_1, and r_2 are the position constant and random number, respectively. To use it in the script file

(MATLAB), a few steps are needed to get the optimized value of the function. As a result, an algorithmic replacement program model is created to find the optimal solution for the parties.

2.2.4. Jellyfish Optimization (JFO). JFO is a new metaheuristic optimization algorithm based on jellyfish behavior. This method is inspired by the exploration behavior and movement patterns of *Jellyfish* [44]. In JFO, the amount of food at different locations varies. Therefore, jellyfish movement occurs by comparing the food proportions in an ocean. Its exploration and exploitation approach helps to reach optimal solutions in less time [32, 44]. A flowchart of the JFO algorithms is shown in Figure 5(b). This algorithm follows these rules for operation.

(i) A "time control mechanism"

(ii) Maximum food availability in that ocean area

(iii) Active and passive motions of jellyfish

The ocean current can be calculated by using the following equation [44]:

$$X_i(t+1) = X_i(t) + \text{rand}\,(0,1) * \left(X'' - 3 * \text{rand}(0,1)\right), \tag{10}$$

where the relevant updated position is determined by $X_i(t+1)$ and γ is the motion coefficient.

Equation (11) [44] is considered to calculate the direction of motion, and equation (12) [44] is used to update the location. In equation (14), $c(t)$ value varies between 0 and 1, c_o is a constant value of 0.5, and t represents the time period at a particular instant [32].

$$|\text{Direction}| = \begin{cases} X_j(t) - X_i(t); & \text{if } f\,(X_i) \geq f\left(X_j\right), \\ X_i(t) - X_j(t); & \text{if } f\,(X_i) < f\left(X_j\right), \end{cases} \tag{11}$$

$$X_i(t+1) = X_i(t) + \gamma * \text{rand}\,(0,1) * (\text{Upper bound} - \text{lower bound}), \tag{12}$$

$$X_i(t+1) = X_i(t) + \text{rand}\,(0,1) * \text{Direction}, \tag{13}$$

$$c(t) = \left|1 - \frac{t}{\text{Max}_{\text{iteration}}}\right| \times 2 * \text{rand}\ 0, 1 - 1. \tag{14}$$

The population initialization is performed by using the following equation [32]:

$$X_{i+1} = a * X_i * (1 - x(i)); \quad 0 \leq X_o \leq 1. \tag{15}$$

The logistic chaotic (X_i) value of i^{th} jellyfish, $X_o \in (0, 1)$, and the value of "a" are chosen as 4.0 [32, 44]. To use it in the script file (MATLAB), a few steps are needed to get the optimized value of the function.

Equation (14) represents the time control mechanism in the JFO, and equation (15) [32] describes the "initialization phase" [32, 44], the first step in JFO optimization. The second step is setting the boundary condition for different functions. The boundary condition is essential so that the jellyfish does not move outside the boundary search area. Equation (16) [32, 44] gives the limit of jellyfish in a search space area or boundary condition to jellyfish [32]. A jellyfish is located at $X_{i,d}$ in the d^{th} dimension.

$$\begin{aligned} &\left\{X'_{i,d} = X_{i,d} - \text{Upper bounds} + \text{Lower bounds}; \quad \text{if } X_{i,d} > \text{Upper bounds}\right\} \\ &\left\{X'_{i,d} = X_{i,d} - \text{Upper bounds} + \text{Lower bounds}; \quad \text{if } X_{i,d} < \text{Lower bound}\right\}. \end{aligned} \tag{16}$$

The best location for the food is determined by the jellyfish, where the quantity of food is more. As a result, an algorithmic replacement program model is created that replicates the ocean jellyfish's search patterns and movement. Due to the $c(t)$ functions, it takes more iterations to track the maximum power, as it must find a new direction in every iteration.

3. Results and Discussion

For the analysis purpose and comparison purposes, two modules of different specifications are taken such as 1Soltech-1STH-215P (case 1) and SolarWorld Industries GmbH Sunmodule plus SW 245 poly panel (case 2) that is available in MATLAB R2021a software. Four modules are connected in series to design a panel. With the help of Minitab software, a regression equation or objective function is obtained in terms of voltage and current values obtained from the P-V curves at STC under step-change of irradiance and PSC condition. For step-change of irradiance conditions, different irradiation values are taken at constant temperatures at different time frames.

A similar environmental condition for STC is considered in the simulation model, having an air mass of 1.5, maximum irradiation of 1000 W/m^{2,} and a fixed temperature of 25°C. For PSC, a set of irradiations is taken and operated simultaneously, and the irradiation dataset values lie between 100 W/m^2 and 1000 W/m^2. The effect of air pressure, dust, humidity, and other losses are neglected in this paper. A simulation model is made with the help of MATLAB software. The panel output is taken in terms of V_{max}, I_{max}, and P_{max}, and the comparison of the optimization algorithm is based on parameters such as maximum iterations, number of populations, number of iterations to achieve the GMPP, execution time (sec), tracking efficiency, and RMSE.

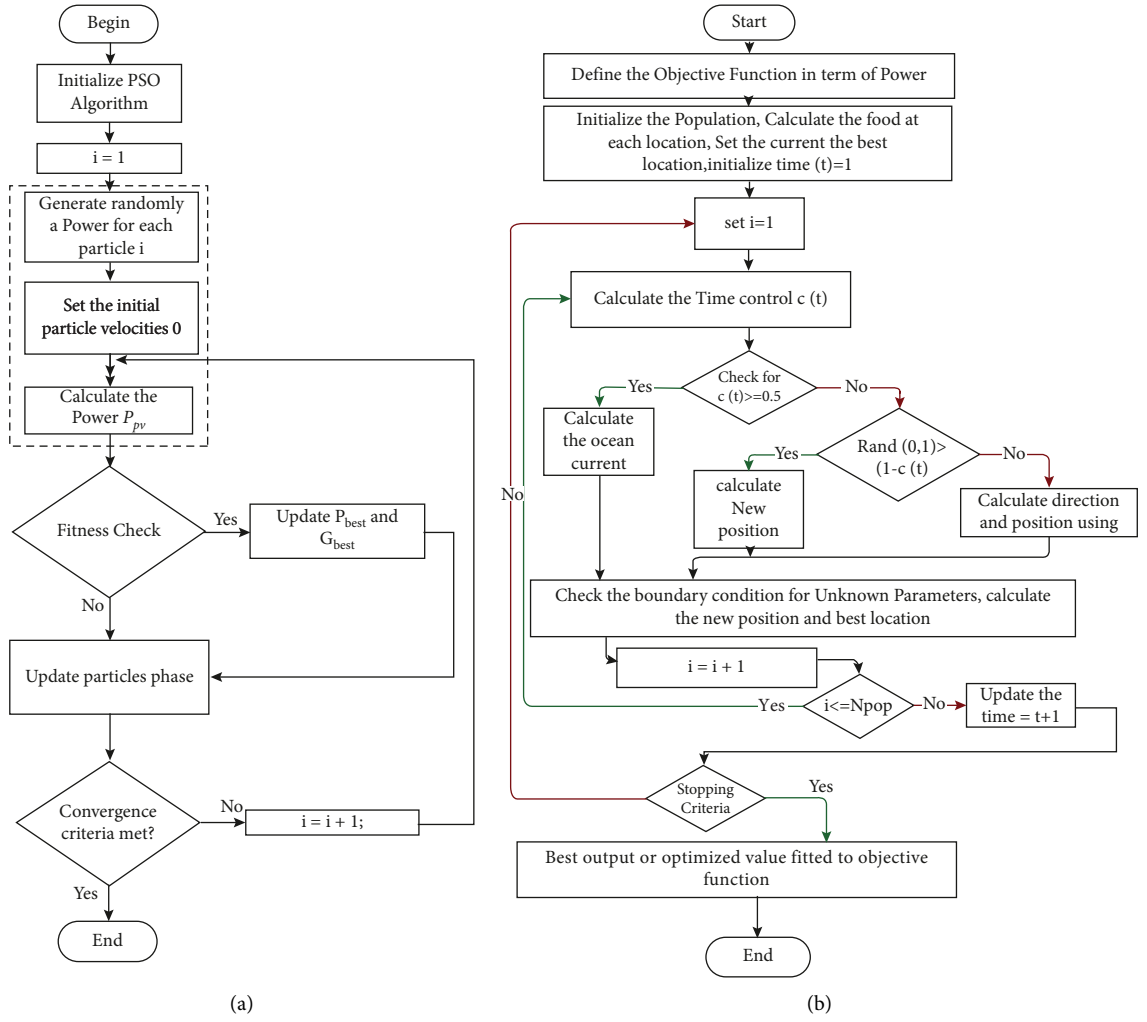

Figure 5: Flowchart for (a) PSO [17] and (b) JFO-based optimization technique [44].

3.1. Case Study 1: 1Soltech-1STH-215P Module. For analysis and comparison purposes, a single PV module of 213.15 watts is considered to form a panel; its specifications are given in Table 2. Four modules are taken and connected in series to form a panel with an output of approximately 852.6 watts, with a maximum voltage and current rating of 116 volts and 7.35 amperes to improve the power rating of the PV system.

The simulation model of a panel (four series connected modules) has irradiation and temperature as input parameters (Figure 6). The irradiation values are taken in such a way that the change in the response (I-V and P-V curves) can be analysed at STC (1000 watt/m^2), and for step-change of irradiance (200, 400, 500, 600, 700, 800, and 1000 watt/m^2) at a constant temperature of 25°C. The I-V and P-V curves for the same is given (Figures 7(a) and 7(b)). The effect of change in irradiation is given in terms of maximum voltage, current, and power (Table 3). The curve at 1000 W/m^2 represents the STC condition of the panel V_{max}, I_{max}, and P_{max} reading for the STC and step-change of irradiances (Table 3 and Figures 7(a) and 7(b)).

From the results, it can be observed that with the change in the value of irradiation, there is a significantly less fluctuation in the V_{max} value, but a significant variation is found in the I_{max} and P_{max} values, which shows that the panel's I_{max} and P_{max} values are more sensitive toward the irradiation value.

Irradiance variations affect the overall performance of solar cells/modules/panels. The power the PV panel receives from the sun varies with the time of the day, which impacts solar cell efficiency and its fill factor (FF). For analysing the effect on the panel under step-change of irradiance, in the model (Figure 6), the irradiation values are changed continuously with the time period of 0, 2, 3, 4, and 5 secs for the irradiation value of 500, 700, 800, and 1000 corresponding to the curves shown in Figures 8(a) and 8(b). In addition, the P_{max}, V_{max}, and I_{max} values are given in Table 3 for the step-change of irradiance conditions. The partial shading condition (PSC) arises when panels are subjected to different irradiation levels caused by nonuniform shading. As a result, the PV array's unshaded module receives higher solar irradiation, while the shaded module receives lesser solar

Table 2: Module/panel (1Soltech-1STH-215P) specification [2].

Parameters	Symbols	Units	Single module specification	Panel specification
OC voltage	V_{oc}	Volts	36.8	147.2
SC current	I_{sc}	Ampere	7.84	7.84
Voltage$_{Maximum}$	V_{max}	Volts	29	116
Current$_{Maximum}$	I_{max}	Ampere	7.35	7.35
Power$_{Maximum}$	P_{max}	Watts	213.15	852.6
İdeality factor	α	—	0.98119	0.98119
Shunt resistance	R_{sh}	Ohm	313.0553	313.0553
Series resistance	R_s	Ohm	0.39381	0.39381

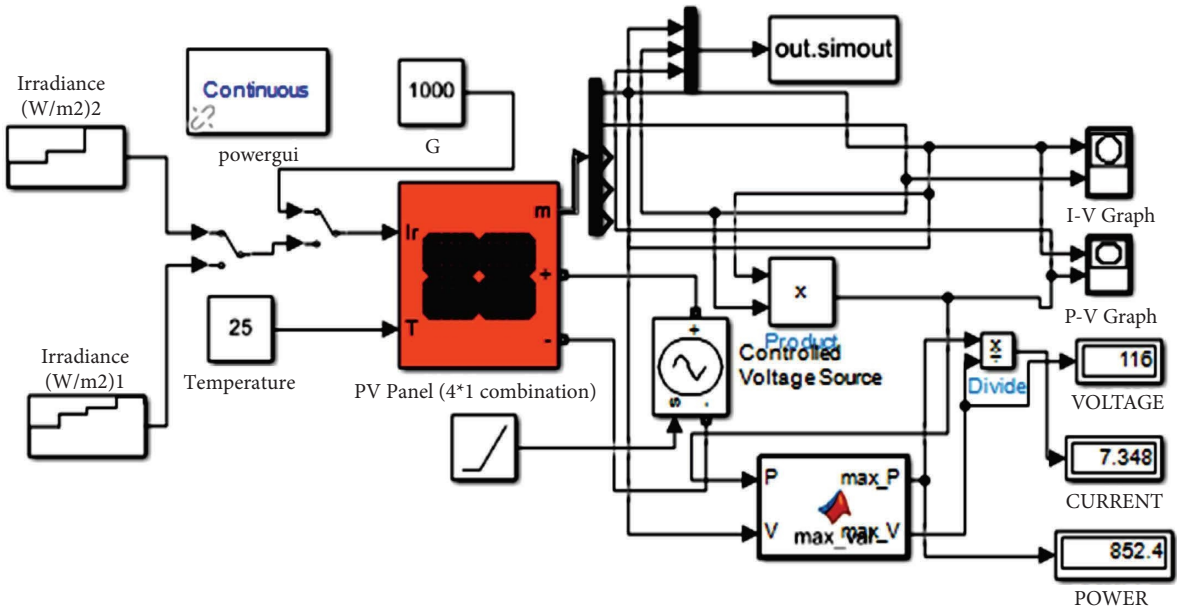

Figure 6: A simulation model of a panel (1Soltech-1STH-215P and SolarWorld Industries GmbH Sunmodule plus SW 245 poly).

irradiation. From an analysis point of view, a panel is designed by connecting four modules (1Soltech-1STH-215P) in series with the help of a bypass diode (Figure 9). Then, its I-V and P-V curves are analysed for PSC. Irradiation values range from 400 W/m^2 to 1000 W/m^2 (Figures 10(a) and 10(b)). In PSC, the input is in terms of irradiation values, and its output is in terms of V_{max}, I_{max}, and P_{max} values (Table 4) for different cases. For case 4, irradiation values of 400, 500, 700, and 1000 W/m^2 have been considered, for which each module is given different irradiation while showing the shading condition. The P-V curve for the PSC condition is shown in Figure 10(b).

Optimization techniques are well-known for solving nonlinear problems under step-change of irradiance and PSC. So, for performance and comparison purposes, a few well-known optimization techniques, such as PSO, GA, ABC, and the proposed JFO technique, are used to track the panel's maximum power. First, the "Minitab" software calculates the regression equation (objective function). The predictor's coefficients, along with the p values, the coefficient of correlation (R), the coefficient of determination (R^2), and the root mean squared error (RMSE) are determined. Summary statistics are taken in terms of R^2, R^2 (adj.), p values, and VIF performance score with the values of 0.9, 0.98, 0.01$e-10$, and 0.23, which shows that the data collected are reliable and regression analysis is possible on the chosen date of the P-V curve. With the help of the regression equation, a MATLAB code is written for different optimization techniques to solve this regression equation calculated for STC, step-changing irradiation, and PSC.

The regression equation values for STC condition, under step-change of irradiance, and PSC condition can be obtained by choosing the voltage and current values as input variables and the output in terms of the maximum power generated at a particular irradiation value. Equation (17) represents the regression equation for the STC taken from the P-V curve for 1000 W/m^2 irradiation (Figure 7(b)). Equation (18) represents the regression equation for the step-change of irradiance values taken from the P-V curve (Figure 8(b)), and equation (19) gives the regression equation for PSC taken from the P-V curve for case 4 (Figure 10(b)).

The regression equation at STC condition is

$$Fx = -1156.53 + 8.02827. * x1 + 146.739. * x2. \quad (17)$$

The regression equation for the condition is

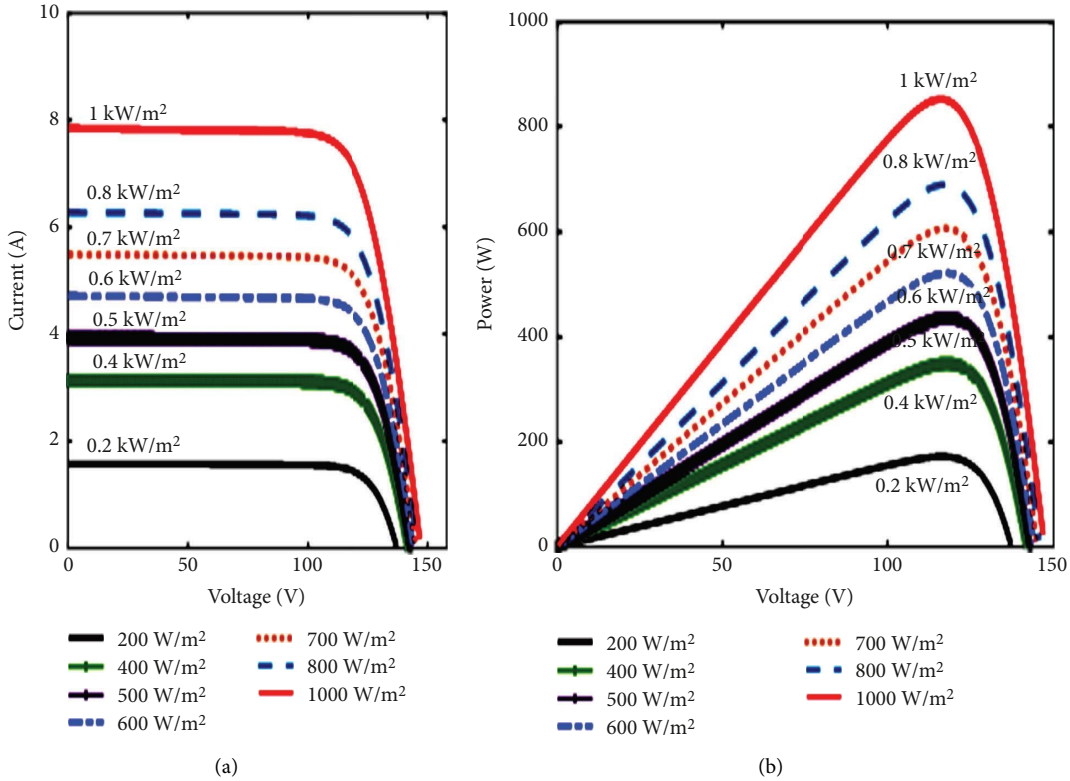

Figure 7: (a) I-V curve. (b) P-V curve under step-change of irradiance (1Soltech-1STH-215P panel).

Table 3: Output values at STC and under step-change of irradiance.

Irradiation (W/m^2)	Max. voltage (V_{max}) (volts)	Max. current (I_{max}) (ampere)	Max. power (P_{max}) (watts)
200	116.35	1.479	172.1
400	117.925	2.956	348.5
500	118	3.692	435.7
600	117.9	4.427	521.7
700	117.525	5.16	606.5
800	117.1	5.892	689.9
1000 (STC)	116	7.348	852.4

$$Fx = -480.50 + 3.6935. * x1 + 121.030. * x2. \quad (18)$$

The regression equation for the partial shading condition is

$$Fx = -689.5 + 5.781. * x1 + 103.32. * x2, \quad (19)$$

where $x1$ represents the voltage and $x2$ represents the current of the PV panel. As per the best knowledge, constant parameters [14, 19, 23, 25, 44] are assigned for different optimization techniques (Table 5). Equations (17)–(19) are the three objective functions for STC, under step-change of irradiance and PSC, that need to be maximized using ABC, PSO, GA, and JFO.

As the parameters are set (Table 5) for ABC, GA, PSO, and JFO, few of the parameters are kept the same, i.e., the number of populations, maximum iteration, and lower and upper limit boundary conditions so that the comparison can be made in terms of maximum power (P_{max}) and the number of iterations at which the maximum power is obtained.

The graphical results and magnified view of maximum power tracked vs. maximum iterations for the different optimization techniques for the STC condition are shown in Figure 11. The response is taken in terms of the maximum iteration at which the maximum power is obtained with the total execution time (Table 6). From the results, it can be concluded that the JFO technique gives the desired maximum power of 851.986 watts in less than 0.0391 sec, with a tracking efficiency of 99.8%. PSO attained the maximum power of 850.987 watts in a time period of 0.0506 sec. Still, it could not track the desired output of the panel, which was 852.4 watts, where ABC takes much execution time (1.0287 sec.) compared to other techniques. From the point of view of overall performance, JFO > PSO > ABC > GA.

The graphical results of the different optimization techniques for the step-change of irradiance conditions are shown in Figure 12. As per the results obtained (Table 7), it can be concluded that the JFO-based optimization technique can track the maximum power of approximately

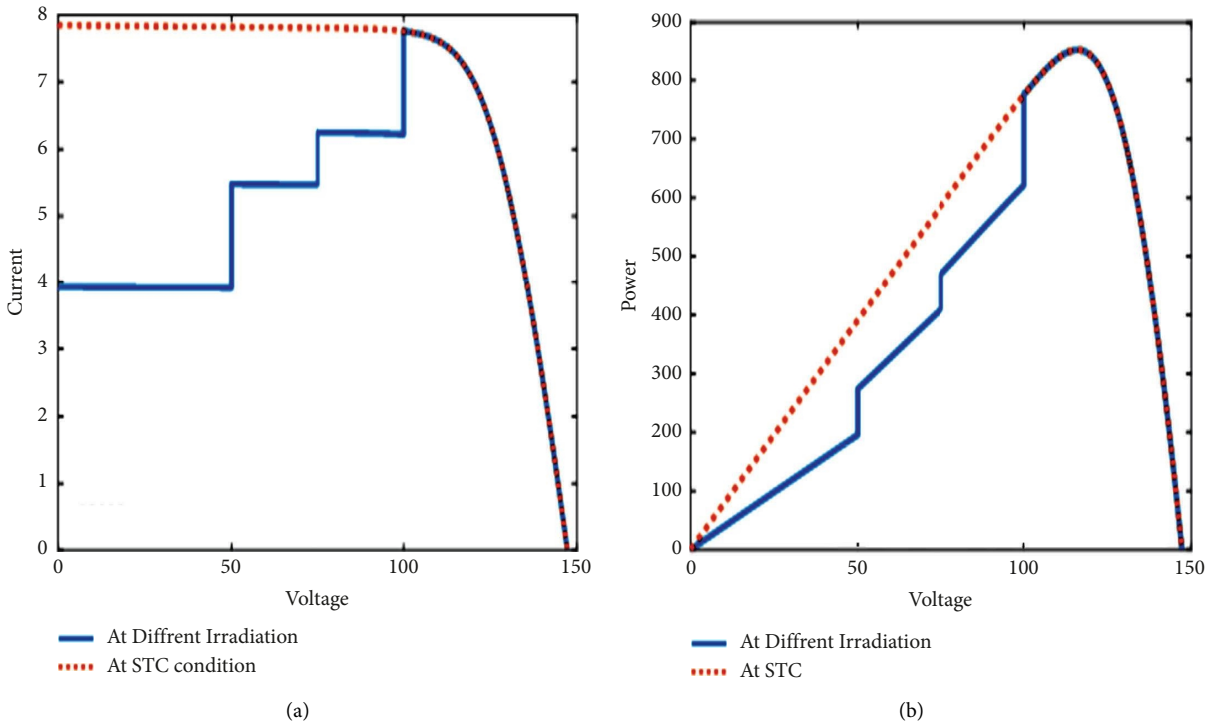

Figure 8: (a) I-V curve and (b) P-V curve at STC and under step-change of irradiance values (500, 700, 800, and 1000 W/m^2).

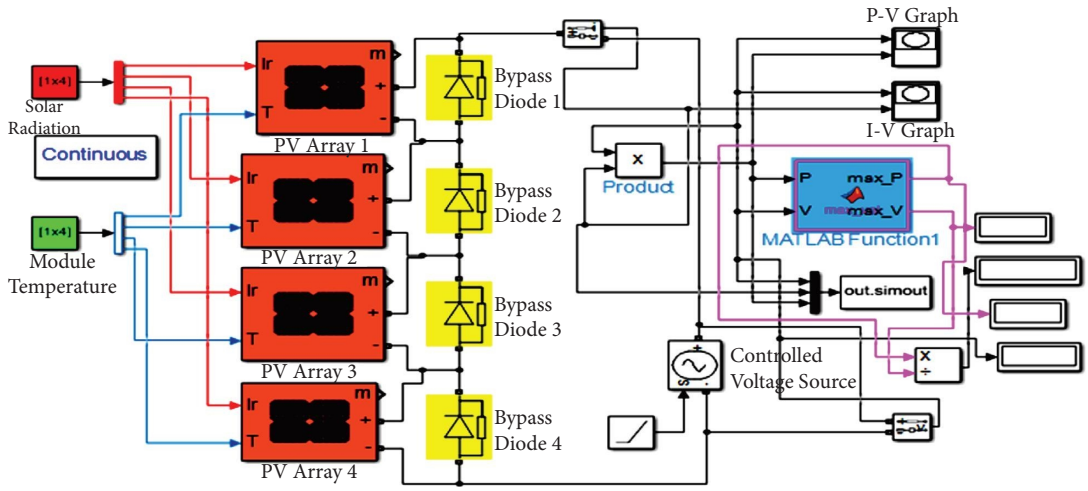

Figure 9: Simulation model for PSC condition for 400, 500, 700, and 1000 W/m^2 irradiation.

835.274 watts with a significantly less time of 0.086 sec. In contrast, PSO was able to track the maximum capacity of 836.114 watts in 10 iterations.

The efficiency of PSO is slightly less than that of JFO, where ABC could track 826.346 watts, and the total executing time of the algorithm was 0.983 seconds, the highest of all algorithms. GA has the least maximum power with an execution time of 0.091 sec. Considering that the tracking efficiency and maximum power are attained in less time, the JFO performance is more accurate and efficient than other optimization techniques. The performance shows the tracking efficiency of JFO > PSO > ABC > GA for step-change of irradiance values.

The partial shading condition can be obtained by taking four series connected modules (Figure 9). To analyse the response of PSC, case 4 has been considered (Figure 10(b)). Equation (19) is the partial shading condition's regression equation or objective function. The response of different optimization techniques is given in Figure 13. The results (Table 8) show that JFO can track the maximum power of 359.460 watts/m^2 in less than 0.1219 sec. In contrast, the execution time of other optimization techniques is more than JFO, and the maximum power is less than JFO. Regarding performance, it can be concluded that JFO can track the maximum power in less time with maximum power tracking efficiency.

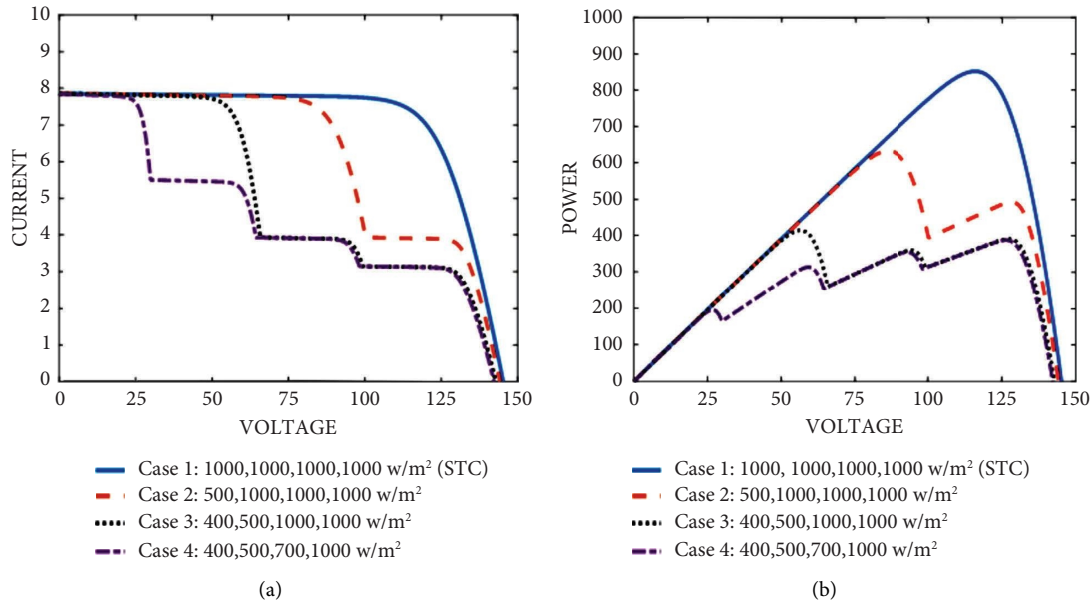

(a) (b)

Figure 10: (a) I-V and (b) P-V curves for PSC for different cases.

Table 4: Output values for 1Soltech-1STH-215P (panel).

Case	Module 1 (W/m^2)	Module 2 (W/m^2)	Module 3 (W/m^2)	Module 4 (W/m^2)	V_{max} (volts)	I_{max} (amp.)	P_{max} (watts)
1	1000	1000	1000	1000	116.05	7.341	852
2	500	1000	1000	1000	86.24	7.339	632.9
3	400	500	1000	1000	56.54	7.324	414.1
4	400	500	700	1000	126.4	3.071	388.1

Table 5: Parameters set for ABC, PSO, GA, and JFO-based optimization techniques [14, 19, 23, 25, 45].

Parameters	Symbols	ABC	PSO	GA	JFO
Dimension	D	2	2	2	2
Lower limit	L_b	0, 0	0, 0	0, 0	0, 0
Upper limit (STC and diff. irradiation, case 1)	U_b	116, 7.348	116, 7.348	116, 7.348	116, 7.348
Upper limit (PSC case 1)	U_b	126.4, 3.071	126.4, 3.071	126.4, 3.071	126.4, 3.071
Upper limit (STC, diff. irradiation, case 2)	U_b	123.2, 7.96	123.2, 7.96	123.2, 7.96	123.2, 7.96
Upper limit (PSC, case 2)	U_b	131.8, 3.22	131.8, 3.22	131.8, 3.22	131.8, 3.22
Number of populations	N_{pop}	8	8	8	8
Maximum iterations	Ite_{Max}	100	100	100	100
Coefficient position update	λ	[−1, 1]	—	—	—
Selection probability	φ	0.5	—	—	—
Cognitive acceleration factor	C_1	—	1.5	—	—
Social acceleration factor	C_2	—	1.5	—	—
Inertia weight	W	—	0.4	—	—
Mutation rate (uniform)	P_c	—	—	0.1	—
Cross-over probability	P_m	—	—	0.9	—
Selection rate	S	—	—	0.1	—
Time control function	C_o	—	—	—	0.5
Logistic chaotic constant	α'	—	—	—	4.0
Motion coefficient	γ	—	—	—	0.1
Distribution coefficient	β	—	—	—	3

3.2. Case Study 2: SolarWorld Industries GmbH Sunmodule plus SW 245 Poly Panel. The panel must operate at its P_{max} point to achieve maximum output in the PV system. Multiple PV modules can be connected in series or parallel combinations to increase the system's power rating to form a panel. The simulation model (Sunmodule plus SW 245 poly panel) of the panel having a single module can obtain the maximum power of 245.168 watts at STC conditions. The SolarWorld Industries GmbH Sunmodule plus SW 245 poly specification for module and panel (four series connected) is

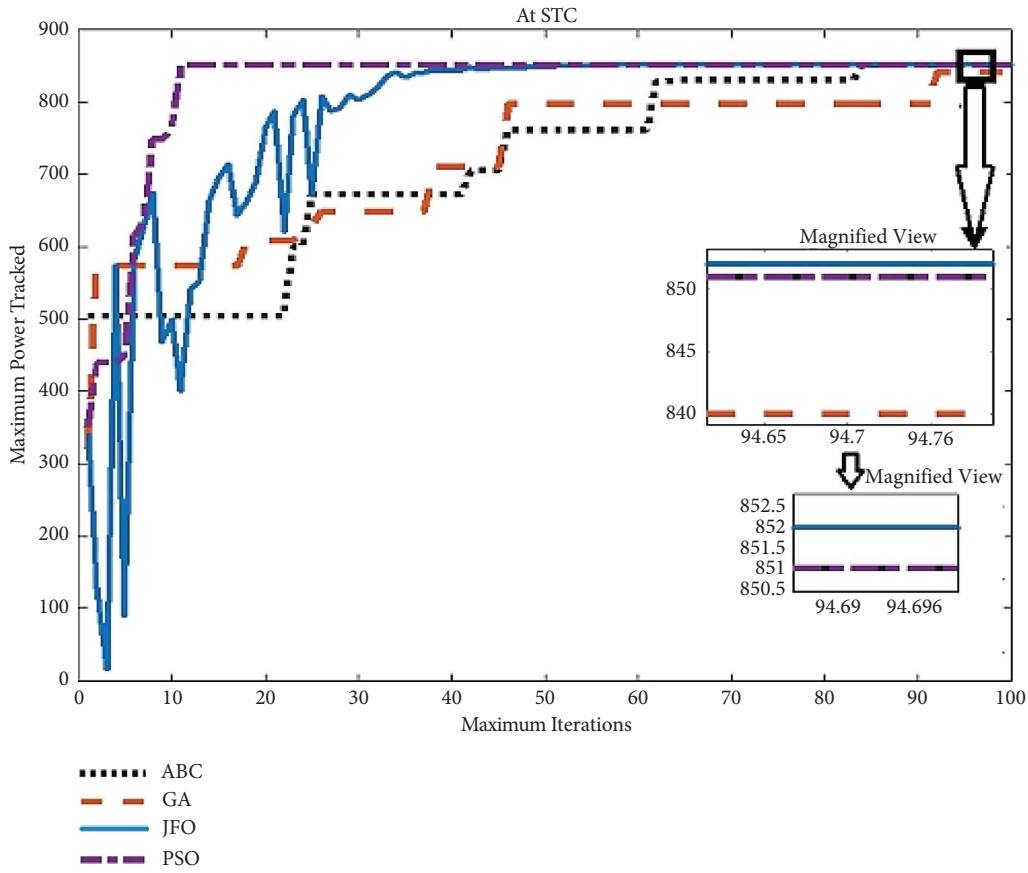

Figure 11: Response of ABC, GA, JFO, and PSO at STC condition (equation (17)).

Table 6: Maximum power and efficiency tracked at STC (Case Study 1).

Algorithm	Max. iteration	Number of population	Number of iterations to achieve the GMPP	Maximum power (watts)	Time (sec)	Tracking efficiency (%)
ABC	100	8	84	850.987	1.0287	99.82403
GA	100	8	92	839.924	0.1107	98.53355
JFO	100	8	68	851.986	0.0391	99.94134
PSO	100	8	11	850.987	0.0506	99.82403

given in Table 9. The I-V and P-V curves for the panel are provided for different irradiation values in Figure 14(a) and 14(b).

We suppose that the configuration (Figure 6) is a four series connected module. In that case, the maximum power tracking capability increases to 980.6 watts with the maximum voltage and current rating of 123.2 volts and 7.96 amps. The response for the single module and the panel (4-series connected) for different irradiation values, i.e., 400, 500, 700, 800, 900, and 1000 W/m^2, is given in Table 10. The maximum power for a panel with a maximum wattage is 980.6 watts. For analysing the panel for step-change of irradiance, in the model (Figure 6), the irradiation values are changed continuously with the time of 0, 2, 3, 4, and 5 secs, for the irradiation values of 500, 700, 800, 1000, and 1000 corresponding to the I-V and P-V curves shown in Figures 15(a) and 15(b). In addition, the panel's P_{max}, V_{max}, and I_{max} values are given in Table 10 for the step-change of irradiance conditions.

A PSC is created by choosing the different irradiations, i.e., 400, 500, 700, and 1000 W/m^2, falling on the panel, i.e., four series connected modules (Figure 9), in such a way that multiple peaks can be obtained in the I-V and P-V curves (Figure 16) if nonuniform irradiation falls on the panel at the same time (shaded). Case 1 refers to STC, while cases 2, 3, and 4 refer to PSC (see Table 11). The PV module should operate at GMP for better panel performance. Cases 1 and 4, which represent the STC and PSC conditions (Figure 16(b)), are analysed.

The regression equation for the STC, PSC, and step-change of irradiance values can be obtained by choosing two input parameters, voltage and current. In contrast, the

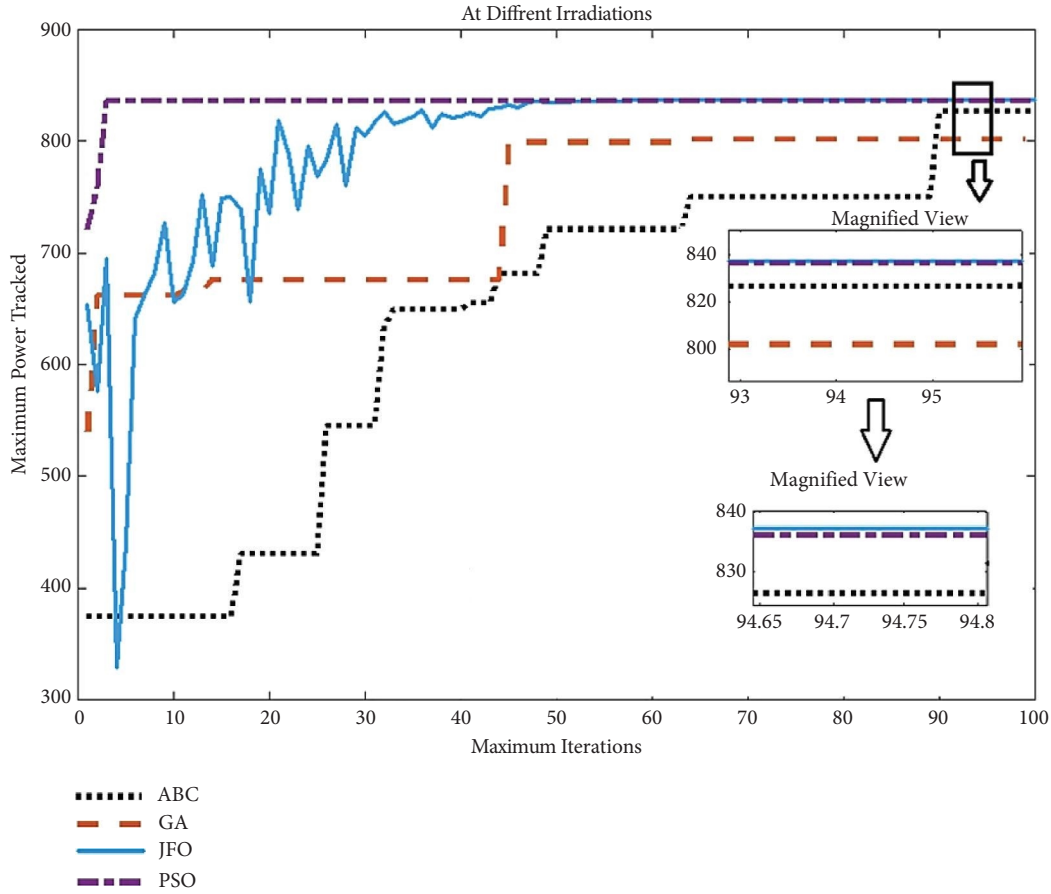

Figure 12: Response of ABC, GA, JFO, and PSO for step-change of irradiance (equation (18)).

Table 7: Maximum power and efficiency tracked at step-change of irradiance (Case Study 1).

Algorithm	Max. iteration	Number of population	Number of iterations to achieve the GMPP	Maximum power (watts)	Time (sec)	Tracking efficiency (%)
ABC	100	8	90	826.346	0.983	96.9
GA	100	8	64	801.989	0.091	94.0
JFO	100	8	81	837.274	0.086	98.2
PSO	100	8	10	835.114	0.2205	97.9

output is in terms of power from the panel. The Minitab software is used to derive the regression equation for STC, PSC, and step-change of irradiances.

Equation (20) represents the regression equation for the STC obtained from the PV curve at $1000\,W/m^2$ (Figure 15(b)). Equation (21) represents the regression equation for the step-change of irradiance values (Figure 15(b)) for the step-change of irradiances condition, and equation (22) represents the regression equation for a PSC from the P-V curve for case 4 (PSC) (Figure 16(b)).

The regression equation for STC is

$$Fx = -1316.06 + 8.6682. * x_1 + 154.483. * x_2. \quad (20)$$

The regression equation for the step-change of irradiance values is

$$Fx = -516.04 + 4.2334. * x_1 + 115.207. * x_2. \quad (21)$$

The regression equation for PSC is

$$Fx = -569.2 + 5.205. * x_1 + 89.97. * x_2. \quad (22)$$

In the abovementioned equations (20–22), $x1$ represents the panel voltage, $x2$ represents the panel current, and Fx is the maximum power obtained from the panel under different environmental conditions. All the dependent parameters for ABC, PSO, GA, and JFO algorithms are given in Table 5, in which many of the parameters are kept the same as it was in case study 1 (1Soltech-1STH-215P module), except the upper limit taken for the case study 2 (SolarWorld Industries GmbH Sunmodule plus SW 245 poly) at STC, PSC, and step-change of irradiances. Voltage and current

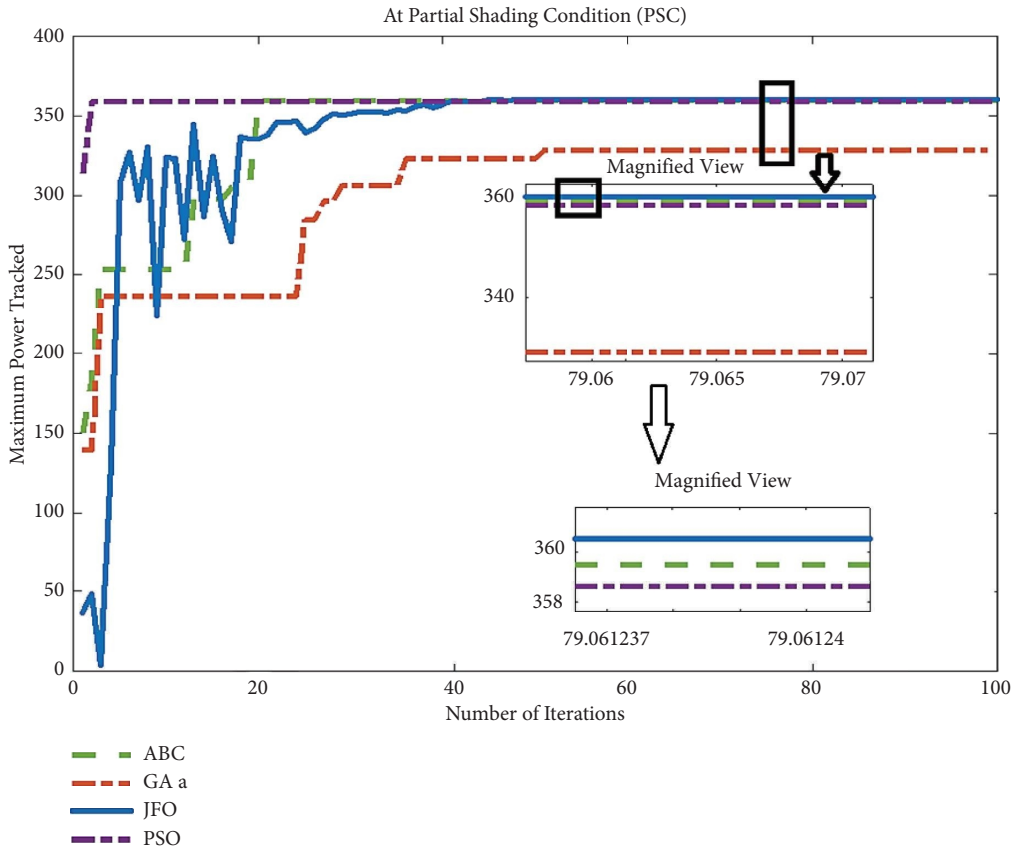

Figure 13: Response of ABC, GA, JFO, and PSO for PSC (equation (19)).

Table 8: Maximum power and efficiency tracked at PSC (Case Study 1).

Algorithm	Max. iteration	Number of population	Number of iterations to achieve the GMPP	Maximum power (watts)	Time (sec)	Tracking efficiency (%)
ABC	100	8	20	358.51	1.0135	98.0
GA	100	8	51	328.4649	0.1300	89.8
JFO	100	8	58	359.4606	0.1219	98.3
PSO	100	8	18	357.633	0.2701	97.8

Table 9: Module/panel specification (SolarWorld Industries GmbH Sunmodule plus SW 245 poly).

Parameters	Symbols	Units	Single module specification	Panel specification (four modules in series)
OC voltage	V_{oc}	Volts	37.5	150
SC current	I_{sc}	Ampere	8.49	8.49
$\text{Voltage}_{\text{Maximum}}$	V_{max}	Volts	30.8	123.2
$\text{Current}_{\text{Maximum}}$	I_{max}	Ampere	7.96	7.96
$\text{Power}_{\text{Maximum}}$	P_{max}	Watts	245.168	980.672
Ideality factor	α	—	1.0531	1.0531
Shunt resistance	R_{sh}	Ohm	352.2121	352.2121
Series resistance	R_s	Ohm	0.24184	0.24184

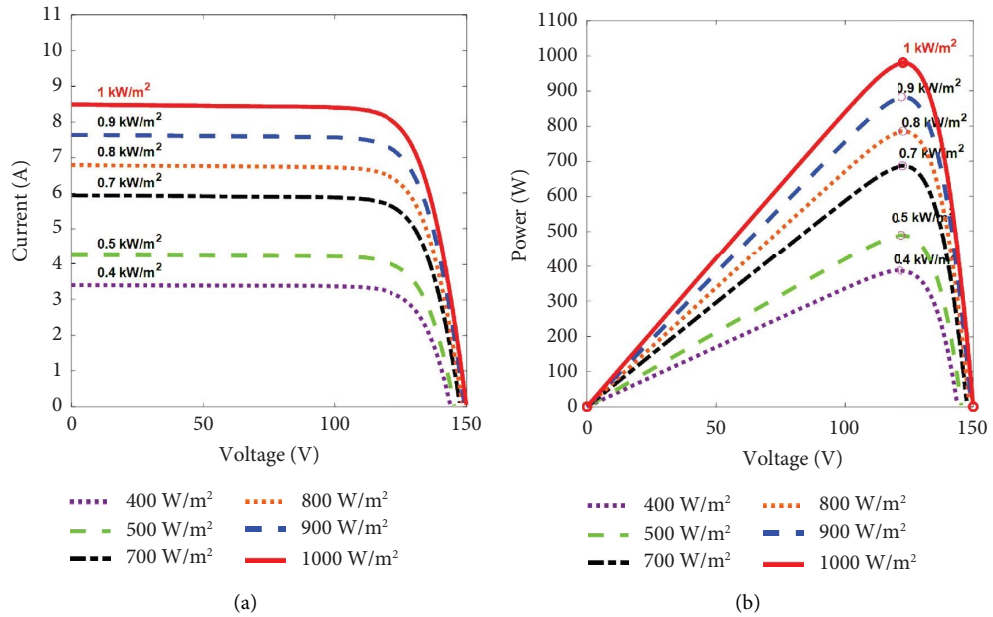

Figure 14: (a) I-V and (b) P-V curves for the SolarWorld Industries GmbH Sunmodule plus SW 245 poly panel (four series connected modules).

Table 10: Output values at different irradiations (SolarWorld Industries GmbH Sunmodule plus SW 245 poly panel).

Irradiation (W/m^2)	Panel (four series connected modules)		
	V_{max} (volts)	I_{max} (amps.)	P_{max} (watts)
400	121.7	3.19	388.2
500	122.4	3.987	487.9
700	123.1	5.578	686.5
800	123.2	6.373	785.2
900	123.2	7.168	883.2
1000	123.2	7.96	980.6

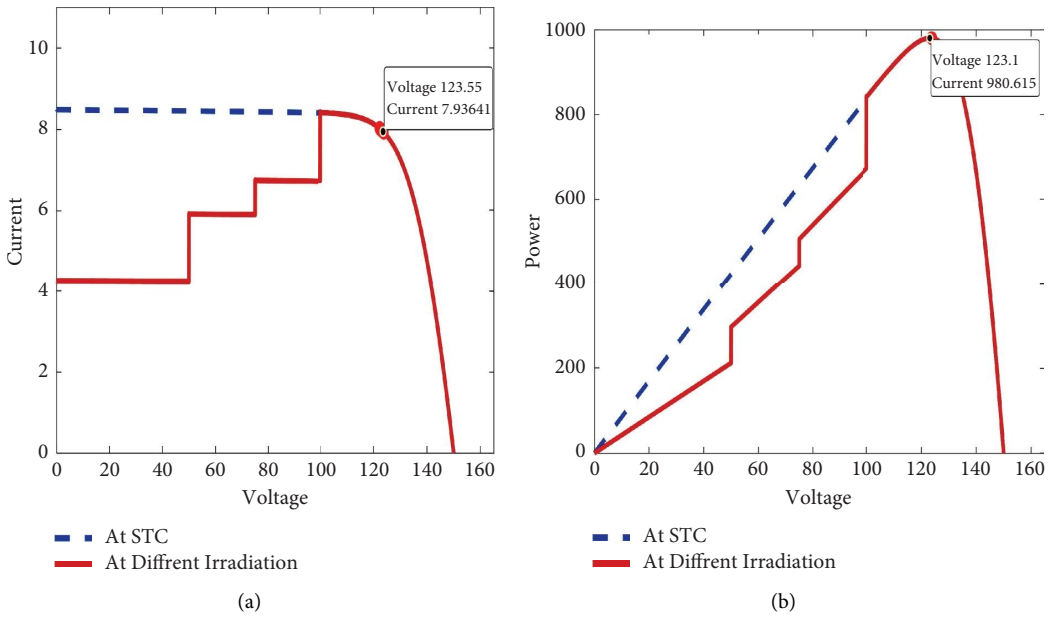

Figure 15: (a) I-V and (b) P-V curves at step-change of irradiance values for SolarWorld industries GmbH Sunmodule plus SW 245 poly panel.

Table 11: Output of P-V curve (SolarWorld Industries GmbH Sunmodule plus SW 245 poly panel).

Case	Module 1 (W/m^2)	Module 2 (W/m^2)	Module 3 (W/m^2)	Module 4 (W/m^2)	V_{max} (volts)	I_{max} (amp.)	P_{max} (watts)
1	1000	1000	1000	1000	123.2	7.96	980.6
2	500	1000	1000	1000	91.68	7.953	729.1
3	400	500	1000	1000	60.16	7.938	477.6
4	400	500	700	1000	131.8	3.22	437.9

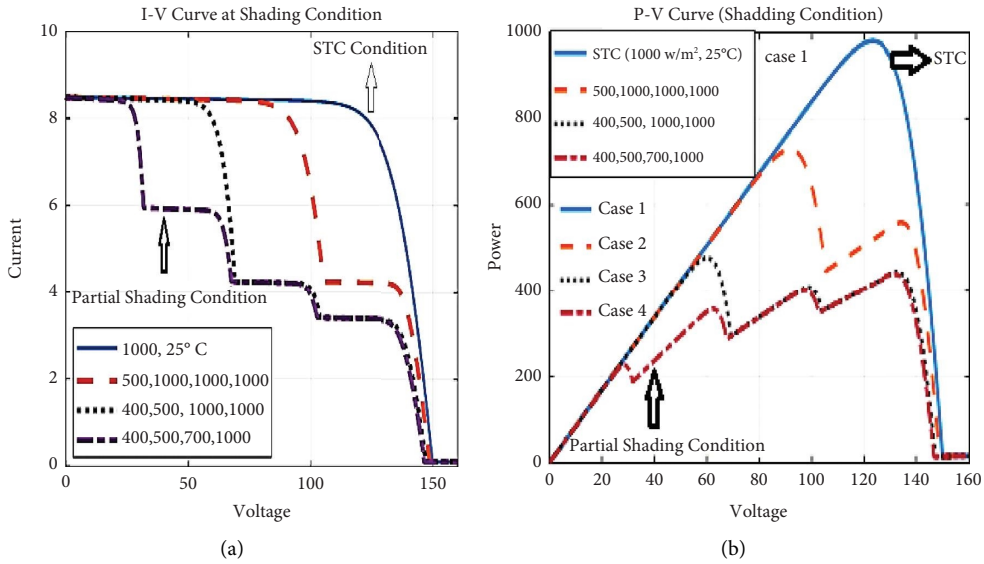

Figure 16: (a) I-V and (b) P-V curves for the SolarWorld Industries GmbH Sunmodule plus SW 245 poly panel showing PSC condition.

values express the upper limit (Ub) at STC, PSC, and step-change of irradiances.

By utilizing equation (20) for the STC condition and putting the parameters of different optimization techniques (Table 5), an optimal solution in terms of maximum power tracked by the panel versus the number of iterations can be plotted for ABC, GA, PSO, and JFO-based algorithms (Figure 17). The response of different algorithms is taken in terms of maximum iterations, number of populations, number of iterations to achieve the GMP, maximum power tracked, time to reach GMPP, and the tracking efficiency (Table 12).

The findings indicate that the JFO approach offers superior tracking performance with much shorter execution times, i.e., 0.0386 sec, to reach the global maximum power point of 980.4 watts, with a total efficiency of 99.9%. However, PSO takes only five iterations. Still, the execution time (0.1233 sec) is higher than JFO and reached the maximum power of 975.992 watts, where ABC's tracking power is higher (979.8014 watts) than PSO, but the execution time (2.1722 sec) is more than PSO. GA was unable to track the GMPP in a given time period. Regarding tracking maximum power, JFO > ABC > PSO > GA. In terms of executing time, JFO > PSO > ABC > GA. Regarding tracking efficiency, JFO > PSO > ABC > G.A. The overall analysis and performance show that JFO is better than PSO, ABC, and GA.

Regarding step-change of irradiances, equation (21) is the regression equation (objective function) used to compare ABC, PSO, GA, and JFO algorithms. The algorithm's response is given in Table 13 and Figure 18. The results prove that JFO is more efficient than the other optimization techniques, PSO, ABC, and GA, in tracking the maximum power of 960.43 watts in less than 0.0767 seconds. PSO and ABC have tracked the maximum power of 958.727 watts and 952.5 watts at 12 and 32 iterations, but they could not track the desired maximum power of 980.6 watts. The findings indicate that the JFO approach offers superior tracking performance with much shorter execution times than other optimization techniques. In terms of overall performance, JFO > PSO > ABC > GA, and in terms of execution time, JFO > PSO > ABC > GA at step-change of irradiance.

In the case of the partial shading condition, equation (22) is the regression equation (objective function) used for all different optimization techniques. PSO, ABC, GA, and JFO responses were obtained as shown in Figure 19 and Table 14. The results prove that the new bioinspired jellyfish optimization technique is more efficient in tracking the maximum power of 415.699 watts with a significantly less execution time of 0.041 sec than the PSO, ABC, and GA. PSO, ABC, and GA have tracked the maximum power of 414.7002 watts, 412.677 watts, and 395.42 at 13, 32, and 97 iterations. Still, they could not track the desired maximum power of 415.7 watts. The results indicate that the JFO performs better than PSO, ABC, and GA. In terms of overall performance, JFO > PSO > ABC > GA. Regarding execution time, JFO > PSO > ABC > GA at PSC.

The overall performance of the JFO was better in both the case studies in all environmental conditions, i.e., at STC, step-change of irradiance, and PSC conditions (Figure 20

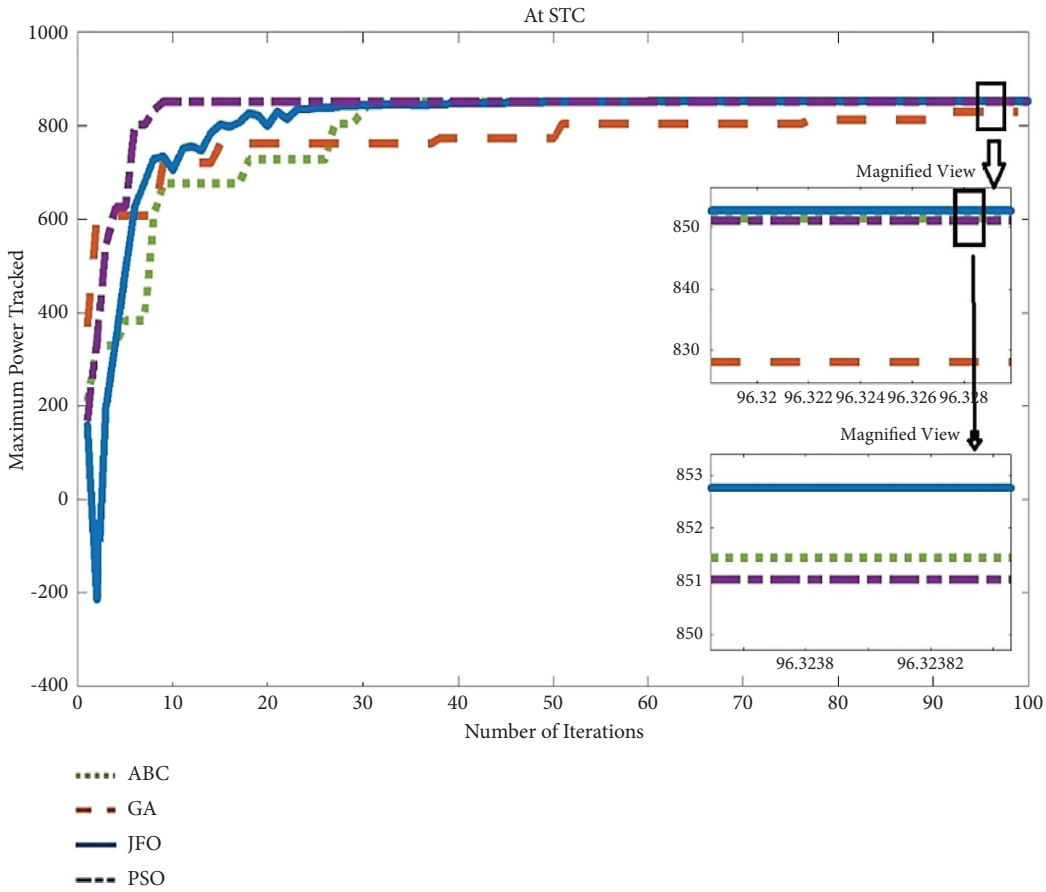

Figure 17: Response of different algorithms at STC (equation (20)).

Table 12: Maximum power and efficiency tracked at STC (Case Study 2).

Algorithm	Max. iteration	Number of population	Number of iterations to achieve the GMPP	Maximum power (watts)	Time (sec.)	Tracking efficiency (%)
ABC	100	8	16	978.8014	2.1722	99.8
GA	100	8	16	926.189	0.1278	94.4
JFO	100	8	83	980.4	0.0386	99.9
PSO	100	8	5	975.992	0.1233	99.5

Table 13: Maximum power and efficiency tracked at step-change of irradiances (Case Study 2).

Algorithm	Max. iteration	Number of population	Number of iterations to achieve the GMPP	Maximum power (watts)	Time (sec.)	Tracking efficiency (%)
ABC	100	8	32	952.5	0.980	97.2
GA	100	8	98	951	0.0386	97.0
JFO	100	8	59	960.43	0.0767	98.0
PSO	100	8	12	958.727	0.0547	97.8

and Table 15). Performance analysis and comparison are made on the following outcome, i.e., maximum power tracked, the execution time of an algorithm, iteration at which the maximum power is tracked, efficiency, and RMSE. The RMSE value of JFO (0.594) is much less than PSO, ABC, and GA (Table 16). Module/panel specifications for testing 1Soltech-1STH-215P and SolarWorld Industries GmbH Sunmodule plus SW 245 poly were considered (Tables 2 and 9). The effect of irradiation on the module/panel for STC, under step-change of irradiance and PSC, is shown in

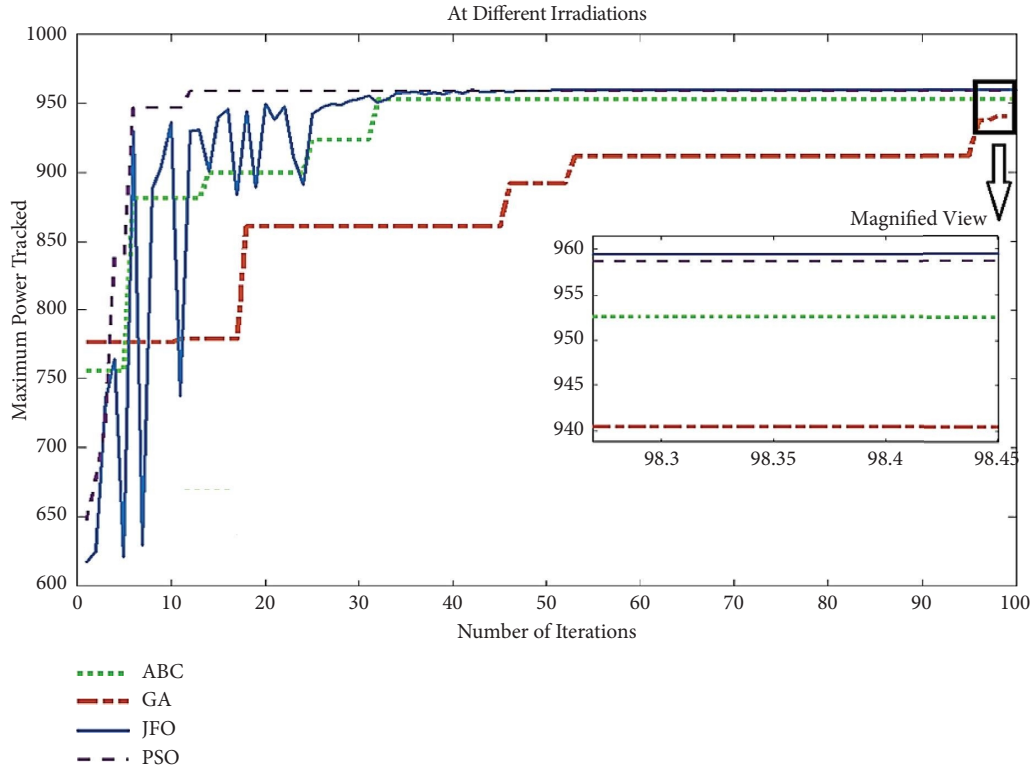

Figure 18: Response of different algorithms for step-change of irradiances (equation (21)).

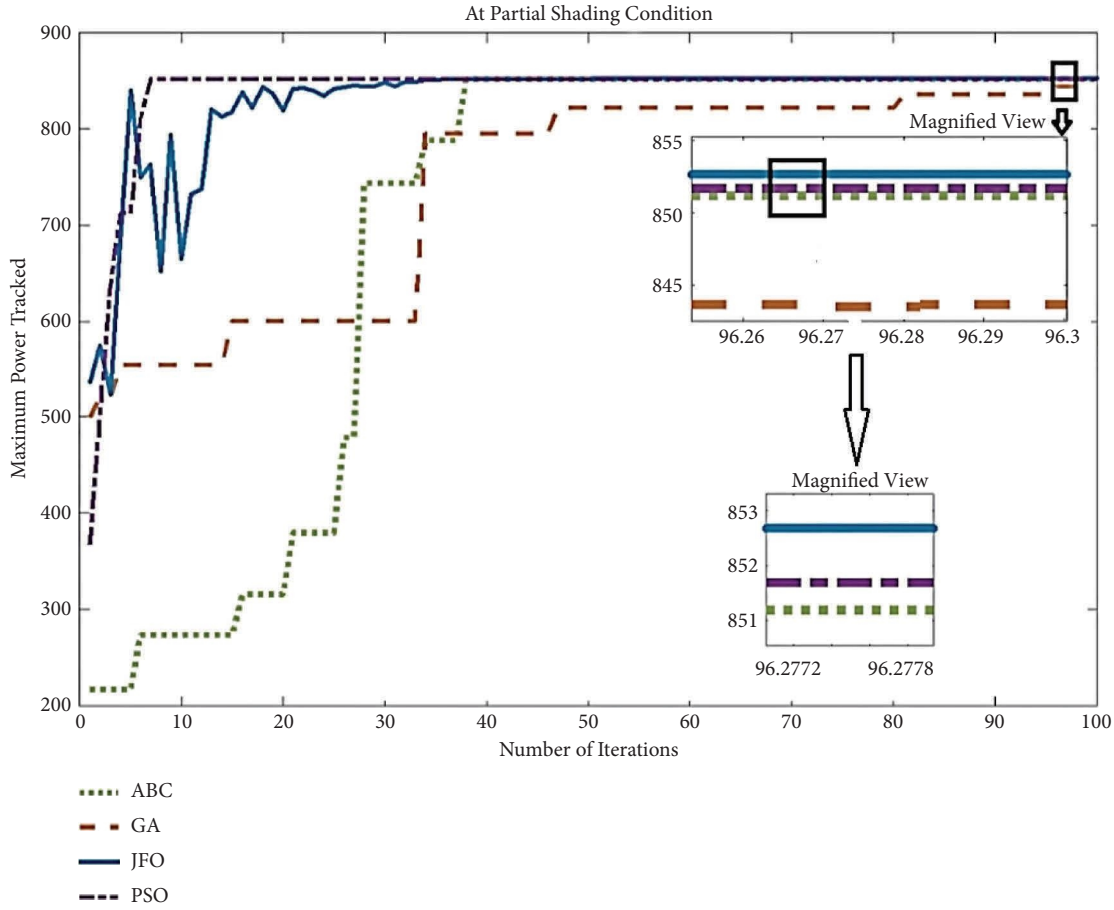

Figure 19: Response of different algorithms at PSC (equation (22)).

Table 14: Maximum power and efficiency tracked at PSC (Case Study 2).

Algorithm	Max. iteration	Number of population	Number of iterations to achieve the GMPP	Maximum power (watts)	Time (sec.)	Tracking efficiency (%)
ABC	100	8	32	412.677	0.877	98.0
GA	100	8	97	395.42	0.175	93.9
JFO	100	8	80	415.699	0.041	98.7
PSO	100	8	13	414.702	0.130	98.5

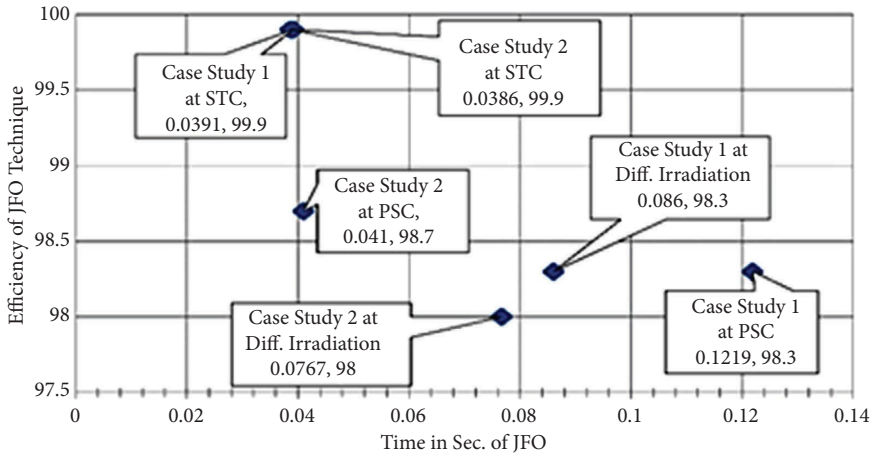

Figure 20: Efficiency vs. time for a different case study with STC, PSC, and step-changing irradiation.

Table 15: Comparison of different algorithms.

	Case study 1: 1Soltech-1STH-215P						Case study 2: Sunmodule plus SW 245 poly panel					
	STC		Under step-change of irradiance		PSC		STC		Under step-change of irradiance		PSC	
	Time (sec)	Efficiency (%)	Time (sec)	Efficiency (%)	Time (sec)	Efficiency (%)	Time (sec)	Efficiency (%)	Time (sec)	Efficiency (%)	Time (sec)	Efficiency (%)
JFO	**0.0391**	**99.941**	**0.086**	**98.2**	**0.1219**	**98.3**	**0.0386**	**99.9**	**0.0767**	**98**	**0.041**	**98.7**
ABC	1.0287	99.824	0.983	96.9	1.0135	98	2.1722	99.8	0.98	97.2	0.877	98
GA	0.1107	98.533	0.091	94	0.13	89.8	0.1278	94.4	0.0386	97	0.175	93.9
PSO	0.0506	99.824	0.2205	97.9	0.2701	97.8	0.1233	99.5	0.0547	97.8	0.13	98.5

Tables 3, 4, 10, and 11. The PSC-supported MPP techniques are compared based on the selection parameters (Table 17), which helps to determine the most suitable method.

The comparison of different optimization techniques, JFO, PSO ABC, and GA, is given for case study 1 (Tables 6–8) and case study 2 (Tables 12–14). From these different comparison tables, it can be concluded that the JFO technique is better than the other three optimization techniques in terms of tracking maximum power, less execution time, and higher efficiency. JFO tracking efficiency in all environmental conditions lies from 98 to 99.9% with a significantly less execution time of 0.0386–0.1219 sec., which proves that the JFO technique can be utilized for tracking the maximum power in all environmental conditions. The JFO technology can also be used for various applications, such as MPPT techniques with converters, stand-alone solar systems, hybrid solar systems with diesel generators, wind turbines, and grid-connected systems.

Findings of other related research work on different PV solar modules are given in Table 16. The results are not compared with other researchers' work because of the different specifications of solar modules from the ones available in the literature. According to the authors in [16, 17], PSO has better fitness value and efficiency than ABC. According to the authors in [14, 43], PSO has a better response than GA. In [11], a comparison between ABC, PSO, and GA has been made, and the ABC algorithm performs better than PSO in tracking speed and efficiency, and PSO shows better response than GA.

As per the study, analysis, and comparison performed in this paper, among the different optimization techniques for obtaining the GMPP with higher efficiency and tracking time, JFO is relatively better in tracking the maximum power with higher accuracy and efficiency, with very less execution time than PSO, GA, and ABC algorithms at step-change of irradiance and for PSC. JFO tracking efficiency in all

Table 16: Finding of other related research work.

Reference	Year	Method	Finding	Comparison based on
Proposed result		GA, ABC, PSO, and JFO	JFO tracking efficiency is 98.7% to 99.99%. In terms of overall performance, JFO > PSO > ABC > GA	*Efficiency* JFO = 98.7% to 99.99% PSO = 97.8% to 99.82% ABC = 96.9 to 99.824% GA = 93.9 to 98.533% *Execution time* JFO = 0.038 to 0.121 sec PSO = 0.123 to 0.2205 sec ABC = 0.877 to 2.172 sec GA = 0.0386 to 0.175 sec *RMSE* JFO = 0.5940 PSO = 3.6330 ABC = 4.684 GA = 33.3639
[18]	2021	ABC and P and O	ABC achieves a much superior performance than P and O	*RMSE* ABC = 0.72, P and O = 0.919
[16]	2022	JAYA, PSO, FPO, CS, and ABC	FPO is more efficient than CS, PSO, and Jaya-based dynamical tracking. Efficiency is better than PSO. ABC method has a shorter tracking time than the PSO	*Tracking time* PSO = 4.1489 sec Jaya = 3.3730 sec FPO = 4.2317 sec CS = 3.7798 sec ABC = 3.8253 sec
[17]	2019	ABC, BAT, GWO, and PSO	PSO has a better response than ABC	*Efficiency* PSO = 96.89% ABC = 90.37% BAT = 95.51% GWO = 94.87%
[24]	2017	PSO, INR, and CS	When compared to PSO, the CS-based tracking was found to be better in all the scenarios. The tracking time of the CS tracker is less than that of the PSO	*Efficiency* CS = 99.90% PSO = 99.87% INR = 99.14%
[27]	2022	P and O, PSO, and SOA	SOA performance is better than PSO	*Efficiency* SOA = 98.05% PSO = 90.60% P and O = 71.35%
[20]	2023	TLABC, PSO, and ABC	The TLABC yields more efficiency and minimum MAE	*Mean absolute error* = 0.13 *Efficiency* = 99.89%

Table 16: Continued.

Reference	Year	Method	Finding	Comparison based on
[15]	2022	PSO, CSA, GWO, MFO, WOA, SSA, and GOA	RMSE of GOA and WOA is less than the rest of the algorithms, which means that the power tracked by these algorithms is dense around the GMPP	*Root mean square error* GOA = 3.9 SSA = 8.8 WOA = 3.9 MFO = 8.5 GWO = 6.8 CSA = 11 PSO = 11.6
[41]	2022	SIOA	The SIOA, with global search ability, can effectively track the GMPP	*Accuracy* SIOA = 99.4428%
[13]	2023	GA, PSO, ABC, DE, CS, GWO, ACO, and M-PSO	A comprehensive review in terms of tuning, convergence speed, complexity, sensing parameters, accuracy, speed, cost, and efficiency	*Efficiency* ABC = 97.75% ACO = 97.87% GWO = 97.8% CSA = high% PSO = 98.1% M-PSO = 99.87%
[14]	2020	ACO, GA, and PSO	PSO-based optimization attains higher tracking efficiency than GA	*Root mean square error* ACO = 0.0021 GA = 0.0010 PSO = 0.0012
[28]	2022	PSO and FPA	PSO and FPA outperform better in PSC, with a difference of 0.53 watts	*Maximum power* PSO = 85.5 W FPA = 86.03 W
[21]	2023	AOA-based PI-IC-MPPT, MIC, GWO, GA, and PSO MPPT	AOA-based PI-IC-MPPT gives better results than MIC, GWO, GA, and PSO	*Reduced rise time and settling time* AOA = 61% and 94% MIC = 3% and 84.7% GWO = 4.5% and 86.6% PSO = 26.9% and 79.3%
[22]	2023	RSA, DOA, GWO, WOA and PSO	RSA gives better efficiency than DOA, GWO, WOA, and PSO	*Efficiency* RAS = 99.85% DOA = 96.43% GWO = 99.63% WOA = 93.37% PSO = 92.63%
[29]	2023	PSO-BOA, PSO, and BOA	PSO-BOA algorithm outperforms the PSO and BOA in terms of convergence accuracy, with a tracking accuracy of 99.94%	*Efficiency/tracking time (s)* PSO-BOA = 99.9/0.47 PSO = 99.89/0.92 BOA = 98.87/0.75

Table 16: Continued.

Reference	Year	Method	Finding	Comparison based on
[33]	2022	DGBCO, DFO, ABC, CS, and PSO	DGBCO < DFO < ABC < CS < PSO	*RMSE* DGBCO = 55.03 DFO = 58.8 ABC = 77.1 CS = 87.7 PSO = 94.7
[45]	2023	SHTS, IABC, GWO, and IABC + SHTS MPPT	IABC + SHTS MPPT shows excellent performance and identifies the GMPP of the PV system with phenomenal rapidity among multiple peaks	*Efficiency* = 99.55%
[34]	2023	EVO, WOA, PSO, CSA, and P and O	EVO-based MPPT controller gives better efficiency than WOA, PSO, CSA, and P and O	*Efficiency* EVO = 100% WOA = 99.86% PSO = 99.75% CSA = 99.31% P and O = 88%
[35]	2023	MRA, WOA, GWO, and PSO	MRA gives better performance than WOA, GWO, and PSO in terms of efficiency and tracking time	*Efficiency* MRA = 99.97 WOA = 99.86 GWO = 99.55 PSO = 99.14 *Tracking time (s)* MR = 0.22 WOA = 0.34 GWO = 0.49 PSO = 0.58
[36]	2023	GRNN-OPA, GRNN-HHO, GRNN-GWO and GRNN-PSO	GRNN-OPA, with an efficiency of 99.96%, settles at GM at 65 ms, which is 71 ms faster than HHO and 45 ms quicker than PSO	*Efficiency* GRNN-OPA = 99.96% GRNN-HHO = 98.24% GRNN-GWO = 97.45% GRNN-PSO = 97.18% *Tracking time (s)* MRA = 0.065 WOA = 0.071 GWO = 0.086 PSO = 0.145

Table 17: Comparison among the PSC-supported methods ABC, GA, and PSO [10, 12, 13, 23, 27, 43].

Properties	GA	ABC	PSO	JFO
Convergence speed	Fast	Fast	Fast	Fast
Complexity	Low	High	Low	Medium
Parameter	V, I	V, I	V, I	V, I
Steady-state oscillation	High	Medium	Medium	Medium
Stability	Stable	Stable	Stable	Stable
Sensitivity	Moderate	Low	High	High
Tracking ability	Medium	High	Medium	High
Economy	Expensive	Low	Medium	Medium
Efficiency	Medium	High	High	Very high
Efficient in PSC	Medium	High	High	High

environmental conditions lies from 98 to 99.9% with significantly less execution time of 0.0386 to 0.1219 sec. As per the result obtained in the paper, the performance of JFO > PSO > ABC > GA proves the effectiveness of the JFO technique over other techniques. As every researcher has used different specifications of panels and different environmental conditions, only a few parameters, such as efficiency, execution time, maximum power tracked, number of iterations needed to track the power, and RMSE, have been considered as the comparison parameters.

Table 17 compares the proposed jellyfish optimization with some existing techniques. Different users have used different parameters and specifications to prove that their technique is better than the existing one, so different comparison parameters are considered such as tracking time [16], RMSE [14, 15, 18], efficiency [13, 17, 22, 24, 27, 29, 31, 34–36], MAE [20], accuracy [41], reduced rise time [21], settling time/tracking time [21, 29, 35], and maximum power [28, 35, 36]. In this paper, maximum power tracked, maximum efficiency, total execution time, convergence speed, complexity, parameter, steady-state oscillation, stability, sensitivity, tracking ability, and economy have been compared [10, 12, 13, 23, 27]; FPA performs better with a small margin than PSO in terms of maximum power [28]. In comparison to a recent 2023 research article [13], M-PSO has the highest efficiency of 99.87, [22] RAS 99.85%, and [29] PSO-BOA 99.7% with 0.47 sec tracking time. As per the proposed JFO algorithm, they have attained the highest efficiency of 99.941% with a tracking time of 0.0386 sec; in terms of RMSE, the error between the predicted and calculated value of JFO was found to be significantly less than 0.5940 in comparison to PSO, ABC, and GA that has been calculated for 100 points at steady-state value (Table 16).

4. Conclusions

This paper comprehensively analyses the bioinspired method used for tracking the GMPP. Comparison and analysis are made under different environmental conditions, such as STC, step-change of irradiance, and partial shading conditions. This paper validates the recently developed jellyfish optimization technique by comparing its performance with PSO, ABC, and GA for smaller population size ($N_{pop} = 8$) for 100 iterations (Ite_{Max}). These algorithms were implemented to track the maximum power for different case studies and environmental conditions. Minitab software was used to obtain regression equation (objective function) and check the data's reliability. Summary statistics are taken in terms of R^2, R^2 (adj.), p values, and VIF performance regression that comes out to be 0.9, 0.98, $0.01e-10$, and 0.23, which shows that the data collected are reliable. Regression analysis is possible on the chosen date of the P-V curves for STC, step-changing irradiation, and PSC. MATLAB/simulation software was used to assess the effectiveness of these algorithms. The comparison and analysis are made in terms of tracking capability, total time of execution, tracking efficiency, accuracy, and RMSE value. The result shows that JFO is relatively better in tracking the maximum power with higher accuracy and efficiency, with significantly less execution time than PSO, GA, and ABC algorithms in all environmental conditions, i.e., at STC conditions, at step-change of irradiance and PSC. The RMSE value of JFO is much less than that of other optimization algorithms. PSO and ABC were close to the desired value of the panel but were less efficient than JFO. GA was unable to track the desired output with higher efficiency. JFO tracking efficiency in all environmental conditions lies from 98 to 99.9% with very less execution time of 0.0386–0.1219 sec. In terms of overall performance, JFO > PSO > ABC > GA. The results obtained from all three cases showed the superiority of the proposed novel algorithm over the other MPPT algorithms.

Abbreviations

ABC: Artificial bee colony
ACO: Ant colony optimization
ALO: Antlion optimizer
AO: Aquila optimizer
AOA: Arithmetic optimization algorithm
AVOA: African vultures optimization algorithm
BOA: Butterfly optimization algorithm
BWS: Black widow spider
CS: Cuckoo search
DE: Different evolution
DGBCO: EVO dynamic group-based optimization algorithm energy valley optimizer
FPO: Flower pollination optimization
GA: Genetic algorithm
GMPP: Global maximum power point
GOA: Grasshopper optimization algorithm
GRNN-OPA: General regression neural network orca predation algorithm

GWO: Grey wolf optimization
HHO: Harris Hawk's optimization
INR: Incremental resistance
I-V: Current-voltage
JFO: Jellyfish optimization
LMPP: Local maximum power point
LFO: Levy flight optimization
MFO: Moth-flame optimization
MRO: Mud ring optimization algorithm
MSFLA: Modified shuffled frog leaping algorithm
NN_ML: Neural network-trained machine learning
P and O: Perturb and observation
PSC: Partial shading condition
PSO: Particle swarm optimization
P-V: Power voltage
RSA: Reptile search optimization algorithm
RMSE: Root mean square error
SIOA: Swarm intelligence optimization algorithm
SOA: Seagull optimization algorithm
SSA: Salp swarm algorithm
SSA: Squirrel search algorithm
STC: Standard test condition
TLABC: Teaching-learning and artificial bee colony
TSO: Tuna swarm optimization
VIF: Variance inflation factor
YSGA: Yellow saddle goatfish algorithm
SHTS: Simultaneous Heat transfer search algorithm
C_1/n_1: Cognitive acceleration factor
C_2/n_2: Social acceleration factor
C_0: Time control function
D: Dimension
I_{max}: Maximum current
I_{sc}: Short-circuit current
Ite_{Max}: Maximum iterations
L_b: Lower limit
N_{pop}: Number of populations
P_c: Mutation rate (uniform)
P_m: Cross-over probability
P_{max}: Maximum power
R_s: Series resistance
R_{sh}: Shunt resistance
S: Selection rate
U_b: Upper limit
V_{max}: Maximum voltage
V_{oc}: Open circuit voltage
W: Inertia weight
A: İdeality factor
α': Logistic chaotic constant
B: Distribution coefficient
Γ: Motion coefficient
Λ: Coefficient position update
Φ: Selection probability.

Data Availability

The data that support the findings of this study are available from the corresponding author upon request. The data are not publicly available due to privacy or ethical restrictions.

Conflicts of Interest

The authors declare that they have no conflicts of interest regarding the publication of this paper.

Authors' Contributions

All authors have contributed to completing the research work and agreed to the published version of the manuscript.

Acknowledgments

The authors thank the Management of Gautam Buddha University, India, for supporting this research.

References

[1] M. K. Singla, J. Gupta, P. Nijhawan et al., "Parameter estimation techniques for photovoltaic system modeling," *Energies*, vol. 16, no. 17, 2023.

[2] D. Yadav and N. Singh, "Comparative analysis of conventional, artificial intelligence, and hybrid-based MPPT technique for 852.6-watt PV system," *International Journal of Social Ecology and Sustainable Development*, vol. 13, no. 2, pp. 1–23, 2022.

[3] N. C. Giri, R. C. Mohanty, R. C. Pradhan, S. Abdullah, U. Ghosh, and A. Mukherjee, "Agrivoltaic system for energy-food production: a symbiotic approach on strategy, modelling, and optimization," *Sustainable Computing: Informatics and Systems*, vol. 40, Article ID 100915, 2023.

[4] D. Yadav, N. Singh, and V. S. Bhadoria, "Comparison of MPPT algorithms in stand-alone photovoltaic (PV) system on resistive load," *Algorithms for Intelligent Systems*, pp. 385–400, Springer Nature Singapore, Singapore, 2021.

[5] R. B. Bollipo, S. Mikkili, and P. K. Bonthagorla, "Hybrid, optimal, intelligent and classical PV MPPT techniques: a review," *CSEE Journal of Power and Energy Systems*, vol. 7, no. 1, pp. 9–33, 2021.

[6] C. H. Basha and C. Rani, "Different conventional and soft computing MPPT techniques for solar PV systems with high step-up boost converters: a comprehensive analysis," *Energies*, vol. 13, no. 2, p. 371, 2020.

[7] M. Chen, S. Ma, J. Wu, and L. Huang, "Analysis of MPPT failure and development of an augmented non-linear controller for MPPT of photovoltaic systems under partial shading conditions," *Applied Sciences*, vol. 7, no. 1, p. 95, 2017.

[8] Y.-J. Zheng, S.-Y. Chen, Y. Lin, and W.-L. Wang, "Bio-inspired optimization of sustainable energy systems: a review," *Mathematical Problems in Engineering*, vol. 2013, Article ID 354523, 12 pages, 2013.

[9] A. Alam, P. Verma, M. Tariq et al., "Jellyfish search optimization algorithm for MPP tracking of PV System," *Sustainability*, vol. 13, no. 21, p. 11736, 2021.

[10] D. Yadav and N. Singh, "Intelligent techniques for maximum power point tracking," *Artificial Intelligence for Solar Photovoltaic Systems: Approaches, Methodologies, and Technologies*, CRC Press (Taylor & Francis), Boca Raton, FL, USA, 2022.

[11] G. Li, Y. Jin, M. W. Akram, X. Chen, and J. Ji, "Application of bio-inspired algorithms in maximum power point tracking for PV systems under partial shading conditions – a review," *Renewable and Sustainable Energy Reviews*, vol. 81, no. part 1, pp. 840–873, 2018.

[12] B. Yang, T. Zhu, J. Wang et al., "Comprehensive overview of maximum power point tracking algorithms of PV systems under partial shading condition," *Journal of Cleaner Production*, vol. 268, Article ID 121983, 2020.

[13] M. Kumar, K. P. Panda, J. C. Rosas-Caro, A. Valderrabano-Gonzalez, and G. Panda, "Comprehensive review of conventional and emerging maximum power point tracking algorithms for uniformly and partially shaded solar photovoltaic systems," *IEEE Access*, vol. 11, pp. 31778–31812, 2023.

[14] H. Vennila, N. C. Giri, M. K. Nallapaneni et al., "Static and dynamic environmental economic dispatch using tournament selection based ant lion optimization algorithm," *Frontiers in Energy Research*, vol. 10, Article ID 972069, 2022.

[15] M. S. Wasim, M. Amjad, S. Habib, M. A. Abbasi, A. R. Bhatti, and S. M. Muyeen, "A critical review and performance comparisons of swarm-based optimization algorithms in maximum power point tracking of photovoltaic systems under partial shading conditions," *Energy Reports*, vol. 8, pp. 4871–4898, 2022.

[16] K. Wang, J. Ma, K. L. Man, K. Huang, and X. Huang, "Comparative study of modern heuristic algorithms for global maximum power point tracking in photovoltaic systems under partial shading conditions," *Frontiers in Energy Research*, vol. 10, 2022.

[17] M. V. da Rocha, L. P. Sampaio, and S. A. Oliveira da Silva, "Comparative analysis of ABC, Bat, GWO and PSO algorithms for MPPT in PV systems," in *2019 8th International Conference on Renewable Energy Research and Applications (ICRERA)*, pp. 347–352, Brasov, Romania, November 2019.

[18] C. Gonzalez-Castano, C. Restrepo, S. Kouro, and J. Rodriguez, "MPPT algorithm based on artificial bee colony for PV system," *IEEE Access*, vol. 9, pp. 43121–43133, 2021.

[19] K. Sundareswaran, P. Sankar, P. S. R. Nayak, S. P. Simon, and S. Palani, "Enhanced energy output from a PV system under partial shaded conditions through artificial bee colony," *IEEE Transactions on Sustainable Energy*, vol. 6, no. 1, pp. 198–209, 2015.

[20] D. K. Kishore, M. R. Mohamed, K. Sudhakar, and K. Peddakapu, "Swarm intelligence based MPPT design for PV systems under diverse partial shading conditions," *Energy*, vol. 265, Article ID 126366, 2023.

[21] M. A. E. Mohamed, S. Nasser Ahmed, and M. Eladly Metwally, "Arithmetic optimization algorithm based maximum power point tracking for grid-connected photovoltaic system," *Scientific Reports*, vol. 13, no. 1, Article ID 5961, 2023.

[22] N. Douifi, A. Abbadi, F. Hamidia, K. Yahya, M. Mohamed, and N. Rai, "A novel MPPT based reptile search algorithm for photovoltaic system under various conditions," *Applied Sciences*, vol. 13, no. 8, p. 4866, 2023.

[23] A. Ali, K. Almutairi, M. Z. Malik et al., "Review of online and soft computing maximum power point tracking techniques under non-uniform solar irradiation conditions," *Energies*, vol. 13, no. 12, p. 3256, 2020.

[24] H. Rezk, A. Fathy, and A. Y. Abdelaziz, "A comparison of different global MPPT techniques based on meta-heuristic algorithms for photovoltaic system subjected to partial shading conditions," *Renewable and Sustainable Energy Reviews*, vol. 74, pp. 377–386, 2017.

[25] S. Javed and K. Ishaque, "A comprehensive analyses with new findings of different PSO variants for MPPT problem under partial shading," *Ain Shams Engineering Journal*, vol. 13, no. 5, Article ID 101680, 2022.

[26] B. Pakkiraiah and G. D. Sukumar, "Research survey on various MPPT performance issues to improve the solar PV system efficiency," *Journal of Solar Energy*, vol. 2016, Article ID 8012432, 20 pages, 2016.

[27] A. Chalh, R. Chaibi, A. E. Hammoumi, S. Motahhir, A. E. Ghzizal, and M. Al-Dhaifallah, "A novel MPPT design based on the seagull optimization algorithm for photovoltaic systems operating under partial shading," *Scientific Reports*, vol. 12, no. 1, Article ID 21804, 2022.

[28] V. R. Krishna Reddy and M. V. Priya, "Partial shaded solar photovoltaic system using particle swarm optimization (PSO) algorithm and comparing with novel flower pollination algorithm (FPA) to enhance power output," in *2022 2nd International Conference on Technological Advancements in Computational Sciences (ICTACS)*, Tashkent, Uzbekistan, October 2022.

[29] Y. Wang, S. Dai, P. Liu, and X. Zhao, "A hybrid particle swarm optimization with butterfly optimization algorithm based maximum power point tracking for photovoltaic array under partial shading conditions," *Sustainability*, vol. 15, no. 16, Article ID 12402, 2023.

[30] M. Alanazi, A. Fathy, D. Yousri, and H. Rezk, "Optimal reconfiguration of shaded PV based system using African vulture's optimization approach," *Alexandria Engineering Journal*, vol. 61, no. 12, pp. 12159–12185, 2022.

[31] N. M.-A. Mutombo and B. P. Numbi, "Development of a linear regression model based on the most influential predictors for a research office cooling load," *Energies*, vol. 15, no. 14, p. 5097, 2022.

[32] A. Khare, G. M. Kakandikar, and O. K. Kulkarni, "An Insight review on jellyfish optimization algorithm and its application in engineering," *Review of Computer Engineering Studies*, vol. 9, no. 1, pp. 31–40, 2022.

[33] S. K. R. Moosavi, M. Mansoor, M. H. Zafar, N. M. Khan, A. F. Mirza, and N. Akhtar, "Highly efficient maximum power point tracking control technique for PV system under dynamic operating conditions," *Energy Reports*, vol. 8, pp. 13529–13543, 2022.

[34] M. Kamran Khan, M. Hamza Zafar, T. Riaz, M. Mansoor, and N. Akhtar, "Enhancing efficient solar energy harvesting: a process-in-loop investigation of MPPT control with a novel stochastic algorithm," *Energy Conversion and Management X*, vol. 21, Article ID 100509, 2024.

[35] M. H. Zafar, M. Abou Houran, M. Mansoor et al., "A novel MPPT controller based on mud ring optimization algorithm for centralized thermoelectric generator under dynamic thermal gradients," *Applied Sciences*, vol. 13, no. 7, p. 4213, 2023.

[36] N. M. Khan, A. Ahmed, S. K. Haider, M. H. Zafar, M. Mansoor, and N. Akhtar, "Hybrid general regression NN model for efficient operation of centralized TEG system under non-uniform thermal gradients," *Electronics*, vol. 12, no. 7, p. 1688, 2023.

[37] A. K. Podder, N. K. Roy, and H. R. Pota, "MPPT methods for solar PV systems: a critical review based on tracking nature," *IET Renewable Power Generation*, vol. 13, no. 10, pp. 1615–1632, 2019.

[38] F. Li, W. Dong, and W. Wu, "A general model for comprehensive electrical characterization of photovoltaics under partial shaded conditions," *Advances in Applied Energy*, vol. 9, Article ID 100118, 2023.

[39] J. Ma, D. Hong, K. Wang, Z. Bi, X. Zhu, and J. Zhang, "Analytical modeling and parameter estimation of

photovoltaic strings under partial shading conditions," *Solar Energy Materials and Solar Cells*, vol. 235, Article ID 111494, 2022.

[40] A. S. Benyoucef, A. Chouder, K. Kara, S. Silvestre, and O. A. sahed, "Artificial bee colony based algorithm for maximum power point tracking (MPPT) for PV systems operating under partial shaded conditions," *Applied Soft Computing*, vol. 32, pp. 38–48, 2015.

[41] J. Li, Y. Wu, S. Ma, M. Chen, B. Zhang, and B. Jiang, "Analysis of photovoltaic array maximum power point tracking under uniform environment and partial shading condition: a review," *Energy Reports*, vol. 8, pp. 13235–13252, 2022.

[42] T. Abuzairi, W. W. A. Ramadhan, and K. Devara, "Solar charge controller with maximum power point tracking for low-power solar applications," *International Journal of Photoenergy*, vol. 2019, Article ID 5026464, 11 pages, 2019.

[43] S. Ahmed, S. Mekhilef, M. B. Mubin, and K. S. Tey, "Performances of the adaptive conventional maximum power point tracking algorithms for solar photovoltaic system," *Sustainable Energy Technologies and Assessments*, vol. 53, Article ID 102390, 2022.

[44] D. Yadav, N. Singh, V. S. Bhadoria, N. C. Giri, and M. Cherukuri, "A novel metaheuristic jellyfish optimization algorithm for parameter extraction of solar module," *International Transactions on Electrical Energy Systems*, vol. 2023, 21 pages, 2023.

[45] L. Gong, G. Hou, and C. Huang, "A two-stage MPPT controller for PV system based on the improved artificial bee colony and simultaneous heat transfer search algorithm," *ISA Transactions*, vol. 132, pp. 428–443, 2023.

[46] P. V. Mahesh, S. Meyyappan, and R. Alla, "Maximum power point tracking with regression machine learning algorithms for solar PV systems," *International Journal of Renewable Energy Resources*, vol. 12, no. 13, 2022.